LA-UR- 94-1750

Title: **An Analysis of Three Nuclear Events in P-Tunnel**

Author(s):
William Fourney, University of Maryland
Richard Dick, University of Maryland
Steven R. Taylor, LANL, Group EES-3, Geophysics
Thomas N. Weaver, LANL, Group EES-3, Geophysics

Submitted to: Milestone Report
H415 Program

DISTRIBUTION OF THIS DOCUMENT IS UNLIMITED

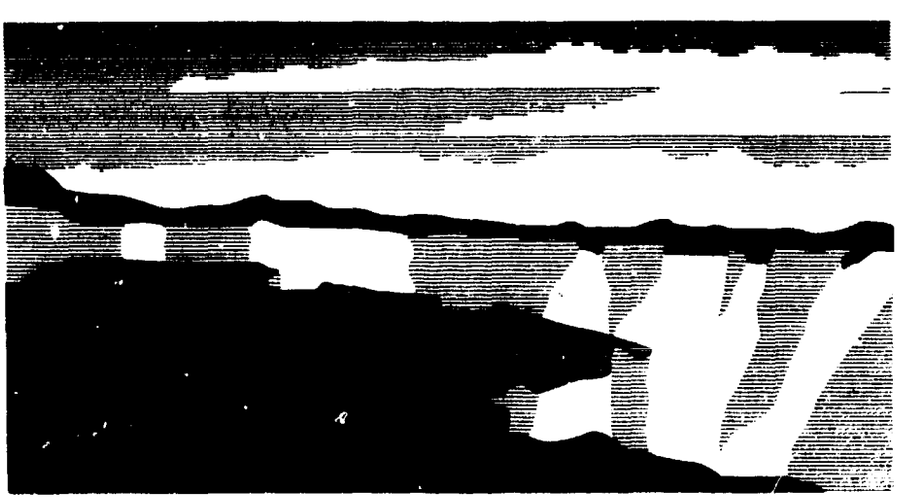

Los Alamos
NATIONAL LABORATORY

Form No. 836 R5
ST 2629 10/91

AN ANALYSIS OF THREE NUCLEAR EVENTS IN P-TUNNEL

WILLIAM L. FOURNEY, RICHARD D. DICK, STEVEN R. TAYLOR

AND THOMAS A. WEAVER

GEOPHYSICS GROUP EES-3

LOS ALAMOS NATIONAL LABORATORY

May 3, 1994

LAUR-94-1750

DISCLAIMER

ABSTRACT

This report examines experimental results obtained from three P Tunnel events - Mission Cyber, Disko Elm, and Distant Zenith. The objective of the study was to determine if there were any differences in the explosive source coupling for the three events. It was felt that Mission Cyber might not have coupled well because the ground motions recorded for that event were much lower than expected based on experience from N Tunnel. Detailed examination of the physical and chemical properties of the tuff in the vicinity of each explosion indicated only minor differences. In general, the core samples are strong and competent out to at least 60 m from each working point. Qualitative measures of core sample strength indicate that the strength of the tuff near Mission Cyber may be greater than indicated by results of static testing. Slight differences in mineralogic content and saturation of the Mission Cyber tuff were noted relative to the other two tests, but probably would not result in large differences in ground motions. Examination of scaled free-field stress and acceleration records collected by Sandia National Laboratory (SNL) indicated that Disko Elm showed the least scatter and Distant Zenith the most scatter. Mission Cyber measurements tend to lie slightly below those of Distant Zenith, but still within two standard deviations. Analysis of regional seismic data from networks operated by Lawrence Livermore National Laboratory (LLNL) and SNL also show no evidence of Mission Cyber coupling low relative to the other two events. The overall conclusion drawn from the study is that there were no basic differences in the way that the explosions coupled to the rock.

1.0 Introduction

Three instrumented nuclear tests, Mission Cyber, Disko Elm, and Distant Zenith, were conducted in the P-Tunnel complex within the past six years. Sandia National Laboratories (SNL) measured stress and acceleration for all three events at scaled ranges of 4 to 170 m/kt$^{1/3}$ horizontally from the source. In addition, Lawrence Livermore National Laboratory (LLNL) and SNL recorded the far-field ground motion at several stations on their seismic networks. The study documented in this report was motivated because of the presumed anomalous ground motion results from Mission Cyber compared to Disko Elm and other N-Tunnel events. The belief was based on interpretations of the measured ground motion values that the Mission Cyber source coupled poorly to the medium. The values measured were lower [Bass, 1975] than ground motion predictions based on N-Tunnel tuff property data. To the contrary, the measured ground motion from Disko Elm (conducted after Mission Cyber) agreed with predictions using N-Tunnel tuff properties.

Our approach to the study included an examination of the core and physical property data obtained from rock at the three event sites, an analysis of the close-in gage data (stress and

acceleration) from all the P-Tunnel tests, and an analysis of the seismic data collected by LLNL and SNL. This report is organized into five sections. After this brief introduction, Section 2 presents results of an examination of the core, a brief review of tuff properties, and the mineralogy of the tuff. Section 3 presents comparisons of the close-in stress and acceleration signals and results of fast Fourier transform (FFT) analysis of the signals. An analysis of the two sets of seismic data for the three tests is presented in Section 4. Finally conclusions based on our interpretation of the results are presented in Section 5.

Figure 1.1 shows a map of the P-Tunnel complex and the mined drifts for the three tests [Containment, 1987, 1989, 1991]. The stratigraphic section for Aqueduct Mesa and the elevations for the events are shown in Figure 1.2. As shown in the figure, all three tests were conducted at approximately the same elevation (1682 m). Mission Cyber, the first test, was conducted in the U12P.02 drift in sub-unit MC-2 of the Paintbrush tuff (labeled T_p in Figure 1.2). Disko Elm, the second test, was detonated in the U12P.03 drift in sub-unit MC-3 of the Paintbrush tuff. Distant Zenith was fired in the U12P.04 drift in sub-unit MC-0 of the Paintbrush tuff. Three vertical exploratory holes were drilled in Aqueduct Mesa, UE12P#01, UE12P#4, and UE12P#6, to characterize the P-Tunnel tuff. These holes are shown in Figure 1.1. Hole UE12P#4 was very close to the working point (WP) for Mission Cyber and provided one of several cores that the authors viewed at the Core Library maintained by the United States Geological Survey at the Nevada Test Site (NTS). Figure 1.3 shows an example of the location of the many holes at the three sites that were cored to evaluate the tuff and then used for emplacement of accelerometer and stress gages.

2.0 Core analysis and tuff properties

The properties assigned to the working points for the three tests are listed in Table 2.1 [Containment, 1987, 1989, 1991]. As noted, the tuff properties are nearly the same at the different WP locations although the actual strata for each were in different subunits of the Paintbrush tuff. At the Mission Cyber WP location the material is described as zeolitized, bedded ash-fall and reworked ash-fall tuff and tuffaceous sandstone [Torres, 1988]. The degree of zeolitization is about 65% [Containment, 1987]. The Disko Elm WP is characterized [Containment, 1989] as the MC-3 subunit and consists of zeolitized, medium grained, calcalkaline ash-fall tuff with scattered silica nodules. The Distant Zenith WP, located in the MC-0 subunit, is described as massive to partially reworked, zeolitized, calcalkaline ash-fall tuff. The degree of zeolitization at the Disko Elm and Distant Zenith WP locations is greater (nearly twice the amount) than at the Mission Cyber WP [Containment, 1991]. Table 2.1 also indicates the mineral constituents of the tuff at each WP [Containment, 1991]. Disko Elm and Distant Zenith had 60% clinoptolite while Mission Cyber had

only 33%. The remaining major constituents for Mission Cyber are 16% smectite and 47% amorphous material. This combination of minerals in the tuff is much greater for the Mission Cyber site than for the other two sites where these constituents amounted to less than 10%. For Disko Elm and Distant Zenith approximately 35% of the tuff consists of opal, quartz, plagioclase, and k-feldspar, while for Mission Cyber these ingredients amount to only 3%. Hence, there are differences in the mineral content between the tuff at the Mission Cyber WP and the WP for Disko Elm and Distant Zenith.

Table 2.1 Working Point Tuff Characteristics

	Mission Cyber	Disco Elm	Distant Zenith
Location	Aqueduct Mesa	Aqueduct Mesa	Aqueduct Mesa
Depth SGZ (m)	270.6	261.2	263.8
Tuff Strata	Paintbrush MC-2	Paintbrush MC-3	Paintbrush MC-0
WP Elevation MSL (M)	1682.4	1682.4	1684.4
Tuff Medium	Zeolitized Ash-Fall Calcalkaline Reworked Ash-Fall Tuffaceous SS	Massive Zeolitized Calcalkaline Ash-Fall	Massive Partial Reworked Zeolitized Calcalkaline Ash-Fall
Bulk Density (g/cc)	1.89	1.91	1.89
Grain Density (g/cc)	2.43	2.45	2.44
Water content (% wet Weight)	18.6	18.9	19.2
Porosity (%)	37	36.7	37.3
Saturation (%)	96	98.4	7.3
Gas-Filled Porosity (%)	1.8	1.4	1.4
P-Wave Velocity (m/s)	2760	2771	3014
Clinoptilolite (%)	33	59	60
Opal (%)	1	3	12
Quartz (%)		3	1
Plagioclase (%)		10	7
K-Feldspar (%)	2	20	13
Illite (%)			2
Smectite (%)	16	5	4
Amorphous (%)	47	2	

We made a qualitative analysis of the core from P-Tunnel to ascertain the quality and strength of the material throughout the stratigraphic section from both vertical and horizontal core. The core from several holes were examined including UE12P.04, U12P.02 IH-1, U12P.03 IH-2, and U12P.04 IH-2 and strength values were assigned in qualitative terms. In general, holes designated with an IH are horizontal instrument holes, those with a U are vertical holes drilled from the upper surface of the mesa, and the hole designated by UE was an exploratory horizontal hole drilled from the tunnel portal prior to the drift being constructed. The core was evaluated according to the apparent strength of the tuff, the density, the porosity, and the appearance. The rock was assigned a strength value based on a scale of zero to ten with the zero being assigned to the sandy, crumbly, weak material and ten assigned to the dense, fine-grained, strongest material. Strength was estimated by how easy or how hard it was to break material from the core, the presence of fine grains or coarse grains, the amount of inclusions large and small, and the tone or sound when the core section was lightly tapped with a metal rod. The density was estimated by hefting sections of the core and comparing the weights among the various sections examined. The porosity was evaluated by how quickly the tuff sections absorbed water. Some of the core was examined twice and some even a third time to establish consistency in the assignment of relative strength. Calibration of the qualitative strength with measured strength data was accomplished using Terra Tek's values from hole UE12P.04 for unconfined and triaxial tests [Torres, 1988]. The average measured strength was correlated to an assigned relative strength value of five.

Figure 2.1 is a plot of relative strength versus depth for the vertical exploratory core hole UE12P.04 which is located very near the Mission Cyber WP. The plot indicates 18 m of weak cap rock, then approximately 116 m of strong tuff, followed by 110 m of weak tuff. At the Mission Cyber WP or the 268 m level and for about 37 m above and 24 m below the WP the tuff relative strength is high (about 7.5 on our scale). There are layers at 18, 225, 292 m, each about 1.5 m thick that consist of sandy unconsolidated material which was assigned a relative strength of between zero and one. The average strength for the entire section is 4.9 and within 60 m of the WP the average relative strength is 5.1. A comparison of relative strength with measured strength is shown in Figure 2.2. The correlation is very good except in the vicinity of the Mission Cyber WP. In an effort to see if the difference between the qualitative analysis and the measure values at the WP was a result of the assigned relative strength, this section of core was examined three times on three separate trips to the Test Site and each time the same relative strength values were assigned.

At this juncture these differences have not been resolved and in our view the tuff in the vicinity of the WP is strong, competent material and hence, good coupling should result. The measurements by Terra Tek, except for the results from two triaxial test, indicates the opposite, that is, the tuff in the vicinity of the working point is relatively weak. This finding should be further

examined by having additional tests conducted on core from the vicinity of the working point.

Several horizontal core holes were drilled for transducers at the tunnel levels for the three events in P-Tunnel. An analyses of one of the three holes for Mission Cyber, U12P.02 IH-1 is shown in Figure 2.3. The tuff had high strength, 5.0 to 7.5, and was consistent over the length of the core. A few weaker layers were observed in each of the holes, but not like those observed for the vertical holes. In addition the tuff within 60 m of the WP was uniform in terms of strength, porosity, and density based on the horizontal core.

A similar analysis was done for the two Disko Elm horizontal core holes which SNL used as instrument holes. In hole U12P.03 IH-2, the tuff has high strength, 7.0, over the length of the core except for a thin layer at 45.8 m from the collar. Generally, the tuff within 60 m of the WP for Disko Elm has a relative strength of 7.0 and the quality is consistently good at the tunnel level over that distance.

A similar analysis was performed for the horizontal instrument holes at tunnel level for the Distant Zenith site. The core from U12P.04 IH-2 indicated good quality tuff with a strength of 6.0 to 7.0 from the WP out to 60 m, similar to that of Mission Cyber and Disko Elm.

Another horizontal exploratory core hole, U12P.06 UG-1, was drilled recently and extends 192 m northward from the U12P.01 drift of the P-Tunnel complex. This core was also examined in a qualitative manner and the results are presented in Figure 2.4. In this hole the tuff quality was noticeably poorer than in other horizontal holes. As indicated in the figure there are many weak layers (relative strength 1.0 to 3.0) mixed with intervals of strong material (relative strength 6.0 to 7.0). One weak section 30 m long in the middle of the core had strengths ranging from 0.5 to 3.5. Other intervals had strength assignments as low as 2.0. The tuff in this horizontal section of P-Tunnel has low quality, many weak layers, inconsistent strength characteristics, and highly variable rock quality in the surrounding 60 meters from the end of the drill hole. These features could affect the manner in which shock/stress waves propagate [Fourney et al, 1993] and hence the ground motion amplitudes would be diminished.

The characteristics of the tuff in the vicinity of the three events in P-Tunnel based on examination of the core show many weak layers in combination with strong layers, especially in the vertical direction. Some of the weak layers are within one wavelength (100 to 150 m) of the stress wave generated by the source and hence reflections from these layers may be superimposed on the initial wave. Consequently the structure of the observed wave form may be modified even though the weak zones may not be in the immediate vicinity of the WP or in the line-of-sight of the gage.

Because of the nature of the strength tests performed by Terra Tek, the specimen material used for the tests was good, high quality lengths of core. No test specimens were selected from the weak, sandy, crumbly layers of tuff because this material will not hold together. Hence, the overall strength data used in the codes and in other interpretive processes may present the tuff as strong

while evidence of the weak zones are missing. In other words there is bias towards a material that is too strong and does not represent the strength variations of the tuff strata.

The tuff characteristics for the three nuclear events are very similar in terms of strength, but there are some differences. For example, the calculated air-filled void of the tuff for the Mission Cyber WP is 1.8 % and is 1.4 % at the other two sites. This is a small difference, but could account for some of the presumed differences in ground motion and stress between Mission Cyber and Disko Elm and N-Tunnel response. Differences in mineral content at each test site is another factor. For example, minerals for the tuff at the Disko Elm and Distant Zenith WP are very similar, but at Mission Cyber the percentages of the major mineral constituents are noticeably different. Perhaps these differences in mineral content and their possible affect on stress wave coupling should be examined in more detail.

3.0 Analysis of Ground Motion Measurements for P Tunnel Events.

3.1 Introduction.

In this section we present an analysis of data taken by scientists from Sandia National Laboratories from Mission Cyber, Disko Elm, and Distant Zenith. The tests were not of the same yield so where comparisons are made the results will be compared in scaled form. At times we will make comparisons of P Tunnel results with results of a similar nature obtained from tests conducted in N Tunnel.

Sandia fielded both stress gages and accelerometers on all three tests. Velocities and displacements were obtained by integration of the acceleration data. Gages were placed at scaled ranges varying from 4 to 170 $m/kt^{1/3}$. The smallest number of measurements were made for Mission Cyber and the largest number of measurements were made for Distant Zenith. We did not have the results from all of the gages fielded but were able to obtain most of the results from ail three tests.

3.2 Measured Results.

Figure 3.1 shows records obtained from a representative sample of stress gages fielded by Sandia on the three tests. These results are for measurements of stress in the radial direction. The gages shown were selected to demonstrate typical scatter and quality that was present in the results obtained. For example - in Figure 3.1a where results are presented from Mission Cyber - the results obtained from the gage at 35.6 scaled meters and the results obtained for the gage at 36.4 scaled meters show that the peak magnitude recorded at the slightly closer gage was more than twice that of gage located only 0.8 scaled meters away.

Figure 3.1b shows results of stress measurements made from the Disko Elm Event. On that

particular test, eleven measurements of stress were conducted at ranges from 14.5 scaled meters to 65.3 scaled meters. At two ranges (26.6 scaled meters and 36.2 scaled meters) two separate readings of radial stress were made at the same location. Excellent agreement was obtained between those two pairs of readings and the resulting points lie almost on top of one another. The result from gage 46-02 located at 36.2 scaled meters, however, was quite different from the result obtained from gage 39-01 located only 2.2 scaled meters away at 33.8 scaled meters. Disagreement is also evident between gage 46-02 (36.2 scaled meters) and 42-01 (2.1 scaled meters away at 38.3 scaled meters). It is not clear which values are correct. Gage 46-02 agrees with 46-04 which is at exactly the same location but disagrees greatly with 39-01 (2.2 scaled meters closer to the shot). Gage 42-01 on the other hand agrees with the results from 39-01.

As indicated earlier, Distant Zenith had more instrumentation installed than either Mission Cyber or Disko Elm. We do not have all of the results but were given a good representative sample of both stress and acceleration values. Figure 3.1c gives stress measured as a function of time for a number of the gages fielded on Distant Zenith. In this case stress records were obtained from a range of about 7.1 scaled meters to a range of 116.2 scaled meters. Shown in the figure are results from two gages located at the same location - 35.6 scaled meters from the center of the source. There was a significant difference between the results obtained for these two gages with one of the gages reading about twice the amplitude of the second gage. Scientists at Sandia noted the presence of faults in the vicinity of both Disko Elm and Distant Zenith. They attribute some of the differences to the presence of these faults. In particular the difference in the two gages just mentioned is attributed to the presence of such a fault.

Figure 3.2 shows representative samples of the readings from the accelerometers fielded by Sandia in the three tests under discussion. These are presented to give an indication of the scatter in the data and the quality of the data obtained. Notice from the figure that the accelerometer signals from both Mission Cyber and Distant Zenith are noisy compared to the signals from Disko Elm.

3.2.1 Times of arrival

We examined all of the data from standpoint of arrival times. We looked at both the arrival time of the first signal and the arrival time of the peak values. If voids, open joints or layers of weak materials are present in the interval between the gage and the working point then anomalies should be present in the arrival time of the first signals. If the pulse shapes are different from test to test or from location to location within the same test, then there should be anomalies in the arrival times of the peaks. The examination of the arrival times is a good check on assuring proper identification of the gages. The time of arrival data can also be used to determine wave speed which serves as a validation of results obtained from sound speed trials.

The result of looking at the time of arrival versus scaled range of the first signal for both

stresses and accelerations from all three tests indicates that all of the data appears to be well behaved except for the result obtained from gage 3934-01 (a stress gage located at a scaled range of 15.7 m/kt$^{1/3}$ in Mission Cyber). The arrival time from this gage was much later than would be expected based upon the gage location and the shape of the signal was also abnormal when compared to the output of other gages from the test. This particular gage recorded stress for 80 milliseconds after detonation and in addition to the late arrival time the amplitude recorded was only about 0.5 kilobars - much lower than expected at that range. The conclusion is that this signal should not be included in further analysis.

A least square fit was performed on the data from each of the tests. The inverse of the slope of these lines gives the average velocity of the signal through the tuff. The velocities vary from 2661 m/s for Disko Elm to 3000 m/s for Mission Cyber. The velocity for Distant Zenith (2934 m/s) lies very close to the Mission Cyber result. These values are in good agreement with the P wave speeds determined from core testing as given in Table 2.1.

Since the shape of the stress pulse is very much different from the shape of the acceleration pulse we expect a different result for peak arrival times for stress than for acceleration. The information on peak arrival times versus scaled range for acceleration is in good agreement with the information on first signal arrival information. A least square fit was found for the results of each of the three tests and little variation was found from test to test. The wave velocities determined from the fit ranged from 2740 m/s for Distant Zenith to 2463 m/s for Disko Elm. The velocity determined for Mission Cyber was 2604 m/s. The information on the arrival times versus scaled range of the peak stress values indicated that a number of the points from the Distant Zenith test and one point from the Mission Cyber test could be suspect. In the Mission Cyber test the gage closest to the source (15.7 scaled meters) had a late arrival time as did all of the Distant Zenith gages located more than 57 scaled meters from the source. Least square fits to the test results indicate that the velocities vary from 2500 m/s for Disko Elm to 1976 m/s for Distant Zenith. The velocity for Mission Cyber was 2330 m/s. Figure 3.3 shows the data points from the Distant Zenith test along with the least square fit from the Mission Cyber and Disco Elm tests. Notice from the figure that the last four data points from Distant Zenith appear to fit well the slope as determined from the other two tests but there appears to be a time shift in the peak signals. Such a time delay could be caused by the signal passing an open fault such as reported by Sandia scientists but these particular gages were not the ones identified by Sandia as being greatly affected by the faults.

Notice from Figure 3.3 that there are three other gages (the ones between 50 and 60 scaled meters in the figure) that appear shifted later in time but not to such an extent as the gages farther out. There are also two other gages at similar locations that are below the least square fit line and therefore have arrival times earlier than those predicted from the results of Mission Cyber and Disco Elm events. It was in this area that Sandia scientists noted the presence of faults. For all gages that

were time delayed we would expect a decrease in stress magnitude but this was not the case. Some of the gages which were located at the same location had stress magnitudes which varied by factors of two and yet exhibited the same time delay in the peak signal arrival times.

As a consequence of looking at arrival times the results from two of the gages that measured stresses in the Mission Cyber event are felt to be questionable. The first of the two suspect gages is at a scaled distance of 15.7 m, identified as gage 3934-01, which is questioned because of a very late time of arrival of first signal. It also happens to have a very low amplitude compared to the other gages fielded on the event. The second gage from Mission Cyber that is questionable is gage 3938-01 which was located at a scaled range of 63.1 meters. It is suspect from the standpoint of a late arrival time of the peak stress value. At least three and as many as eight of the gages in Distant Zenith test could be questioned based upon the arrival of peak stress data. A similar delay was not seen in peak acceleration arrival time for companion gages - that is for acceleration gages located in the same package. Only the one gage from Mission Cyber (3934-01) is dropped from the data base at this time. The others will be retained but special attention is given to the results when comparing them to the other data.

3.2.2 Stress magnitudes

Figure 3.4 is a comparison of the stress magnitudes measured in the three P Tunnel events. Points marked with a "1" are from Distant Zenith. Those marked with a "2" are Mission Cyber and the 3's are from Disko Elm. (This code will be utilized in all figures presented in this report.) The heavy solid line in the figure gives the location of plus one standard deviation from the mean line for the results of Distant Zenith and Disko Elm. The lower dashed line gives the location of the minus one standard deviation for the same data sets. The light solid line gives the mean of all of the data from all three test taken as a data set. The light solid line running through the two open squares indicates what would be expected from earlier tunnel testing. These results indicate that the data from Disko Elm has very little scatter and in general seem to be higher than those from the other two tests. The results from Distant Zenith are scattered with one point falling on the plus one standard deviation line but with many points being lower than the Disko Elm values and a number of points falling even below the Mission Cyber results. The results from Mission Cyber show little scatter but all points fall on the lower edge of the scatter band. At shorter ranges the measured behavior in P Tunnel is about what would have been expected. At longer ranges the results from P Tunnel lie well below what would have been expected from results obtained from other tunnel testing.

3.2.3 Acceleration magnitudes

Figure 3.5 gives a comparison of acceleration results from the three P Tunnel tests. Again both plus and minus one standard deviation limits for the Disko Elm and Distant Zenith are shown,

as well as the mean line for all three tests, and the expected results based on previous testing in other tunnels. The data from both Mission Cyber and from Disko Elm show little scatter. The data indicate that smaller values of acceleration at any given range were measured for Mission Cyber than for either Disko Elm or Distant Zenith. From the figure it is clear that there is considerable scatter in the data from Distant Zenith. Notice that three of the Distant Zenith results fall on or above the plus one standard deviation limit. Note also that three points from Distant Zenith also fall on or below the minus one standard deviation limit - but even these are slightly higher than the results from Mission Cyber. Again, the P Tunnel response curve lies on the prediction curve at lower ranges and below the prediction curve at larger ranges.

3.2.4 Velocity and displacement

Figure 3.6 presents the velocities that were determined from integration of accelerometer measurements made in Mission Cyber, Disko Elm, and Distant Zenith. As would be expected the scatter in the Distant Zenith acceleration data carries over to the velocity data. Again, the upper and lower limits for one standard deviation to the least squares fit to the Disko Elm and Distant Zenith data are shown as well as the mean for data from all three P Tunnel tests and the expected response from previous tunnel testing. The Mission Cyber data for velocity does not seem to be any farther from the mean than some of the data from Distant Zenith. The data from Mission Cyber is again on the lower edge of that band whereas the Distant Zenith data is located on both the upper and the lower side of the mean. The response curve from P Tunnel testing has about the same slope as the response curve obtained from testing in other tunnels (marked at the ends by open squares) but lies somewhat below that curve.

The scaled displacements obtained from a second integration of the accelerometer indicates that the displacements from Mission Cyber are considerably lower than those obtained from Disko Elm and from Distant Zenith. Figure 3.7 gives a comparison of the dynamic (peak) scaled displacements recorded in Mission Cyber and Disko Elm with the permanent displacements measured in the vicinity of the Mission Cyber test. The points marked with an asterisk represent permanent displacements measured from the Mission Cyber event. These permanent displacements are obtained from a survey of fixed markers upon reentry after the test is conducted. The peak dynamic scaled displacements from Mission Cyber (filled squares) are not much larger than the permanent ones and one point appears to fall below the dynamic value. It would be expected that the dynamic displacement would all be well above the permanent ones since any elastic action between the working point and the measurement location would return to zero before the permanent displacement are measured.

3.2.5 Pulse widths and rise times

It was thought that looking at the waveforms in several different ways would be helpful in determining if there were any differences in the three P Tunnel tests. We decided to look at acceleration measurement rise times, pulse widths, and the ratio of the peak values to the pulse width. For the stress measurements we looked only at rise times, since the stress gages tended to fail before the signals returned to zero and the pulse width would be difficult to determine. Figure 3.8 presents the data and least square fits to the data for widths of the first acceleration pulse as a function of arrival time for all three of the P Tunnel tests. There is a tendency for the width of the acceleration pulse to increase with time of arrival (or equivalently with range). It is evident that the pulse widths at a given scaled range for Distant Zenith are considerably greater than for the other two events and that the Mission Cyber pulse width at a given scaled range is slightly greater than the Disko Elm pulse widths.

We also calculated the ratio of the peak acceleration to the pulse width for the three events. The peak-to-pulse width ratio decreases with increasing time of arrival (or range) in all three events. The ratio of peak acceleration-to-pulse width appears to be greatest for Disko Elm and the results for Mission Cyber and Distant Zenith appear to be intermixed - especially at larger ranges - and to be only slightly less than those for Disko Elm.

Figure 3.9 presents least square fits to the rise time (time required to go from 10% to 90% of the peak acceleration) from all events. As was true with the pulse widths, there appears to be a definite separation in the data. The Distant Zenith results exhibit a larger rise time at a given scaled range. Disko Elm has the smallest rise times. At smaller scaled ranges the data from Mission Cyber and Distant Zenith are in agreement while at larger scaled ranges the Distant Zenith result is well above both the Mission Cyber and the Disko Elm results which are in agreement.

The rise time of the stress pulse increases with range for the three tests. This increase with range is as expected and the results from all three tests appear to be intermixed -indicating similar response from all three test sites.

The conclusion drawn from looking at the wave shapes in this fashion is that there appears to be differences between the three tests from the standpoint of rise times and pulse widths of the acceleration data. The wave forms measured by the accelerometers in Distant Zenith appear to have longer rise times and to also have longer pulse widths than do the accelerometer measurements made in Disko Elm and Mission Cyber. The wave forms measured by the stress gages in the three events, on the other hand, do not show any significant differences.

3.2.6 Rebound time

One of the response features thought to be different between Mission Cyber and other events in P and N Tunnel is the rebound time. The rebound time is defined to be the time at which material

begins to move back towards the center of the detonation and is easily determined by examining the particle velocity at any given range. The rebound time is the time when the velocity first returns to zero and begins to become negative. Figure 3.10 shows a typical velocity obtained from one of the P Tunnel tests. The point marked RB1 is the rebound time - the time when material particles located at the gage position begin to move back towards the source. We also studied the time when this initial negative velocity ended, that is, the time when the velocity again reached zero and became positive (labeled RB2 in the figure). All of the analysis up to now has dealt with the first pulse of the acceleration and stress signals. The rebound times, however, provide information about the later time behavior of the wave as it responds to the tuff. For example the second rebound time (RB2) is determined by information from the accelerometer record well past the first pulse.

In Figure 3.11a a comparison is made for the rebound time RB1 for the three P Tunnel tests and for Hunter's Trophy (a test conducted in N Tunnel). The start of inward velocity from Disko Elm lie above the results from the other two tests - but not greatly above. The data from Mission Cyber appear to lie at the bottom edge of the scatter band - especially at larger ranges and implies that for a given range that the material begins to return towards the center of detonation a little quicker than for the other two tests (with the exception of one location from Distant Zenith at about 60 scaled meters). The data from Hunter's Trophy appears to agree well with the rebound times for Mission Cyber.

With regard to the time at which the velocity again becomes positive (moves away from the source) the results for the three P Tunnel tests are about the same as those for the start of rebound - except there appears to be a little more mixing of the data. The mixing of the data and the lack of data for some tests at the lower ranges makes it difficult to state if there is a significant difference in rebound times among the three P Tunnel events. In general, data from Disko Elm seems to bound the top of the scatter band and results from Mission Cyber the bottom. However, the scatter is enough to prevent a definite statement about separate trends for any of the three events. The end of rebound time for Hunter's Trophy, however, appears to be significantly greater than for all three of the P Tunnel tests. The times for end of inward travel for Hunter's Trophy are 33 to 50 percent greater than the results from the P Tunnel tests. Since the start of rebound times for Hunter's Trophy are as low or lower than for the P Tunnel tests and since the end of rebound times are the greatest for Hunter's Trophy then significant more inward motion should have occurred for Hunter's Trophy compared to the P Tunnel events. Figure 3.11b shows the time duration of the velocity towards the source for the three P Tunnel tests and for Hunter's Trophy. The times for the P Tunnel tests are all at or below 100 milliseconds (scaled) while those for Hunter's Trophy are all around 200 milliseconds.

3.2.7 Area under stress pulse

Stress versus time curves were integrated to obtain "impulse" changes that occur as the pulse propagated into the geologic media. Theoretically, impulse is obtained by integrating the force-time curve. Since force equals stress times area, the integration of the stress time curve should give a suitable picture of changes that occur as the pulse propagates away from the source.

This integration is difficult to perform since the stress values do not normally return quickly to zero and in some cases (if the lead wires are not broken) remain above zero for many tens of milliseconds after the signal arrives. For the stress signal a judgment was made to only integrate for a given time after peak stress arrival which was long enough to ensure that the stress level had returned to a steady level. If the signal returned to zero quickly the signal was only integrated to that time - but such behavior might indicate that the results are not valid. Figure 3.12 presents the results of the integration where scaled impulse is plotted as a function of scaled range. The data from Distant Zenith are scattered significantly but are above similar data from Disko Elm and Mission Cyber. This implies that the impulse obtained from integration of the stress data from Distant Zenith is in all cases larger than impulse obtained in either of the other two tests. The lines shown on the figure are least square fits to the data.

In theory the impulse versus scaled range result should agree from test to test. In fact the scaled impulse versus range curve should be an excellent way of comparing source strengths from one test to the next. The problem of the disagreement could lie in the inability to integrate all of the data over a sufficiently long time due to gage failures.

3.2.8 Fast Fourier transform comparisons

We investigated the various measurements made during the P Tunnel events using spectral analysis to determine differences in behavior. Figure 3.13 shows results from a FFT on two of the accelerometer records from the Distant Zenith event. We performed FFT analysis on all of the stress and accelerometer records available in digital form and compared three different measures from the resulting analysis - the peak amplitude, the corner frequency, and the roll off frequency. The peak amplitude is the maximum amplitude at any frequency and the corner frequency is the frequency where the amplitude begins to decrease. The roll off is the slope of the decreasing portion of the spectrum (the number of decades of decrease in amplitude for a decade change in frequency).

With regard to the stress records, the peak amplitudes were found to be between 0.0006 and 0.04 Kbar sec and the overall trend seemed to indicate a slight decrease with scaled range. The roll off from the various stress measurements was found to be between -0.7 and -2.4. The corner frequencies for the stress data was found to be between 5 and 90 Hz. For all three measures there was a complete intermixing of the data from the three tests and none of the gages appeared to be outside the pattern from the results for the tests taken as a whole. The results of the FFT analysis of

the stress measurements therefore did not reveal any suspicious behavior.

With regard to the acceleration measurements, the corner frequencies were found to range between 8 and 90 Hz. This is about the same as observed in the stress measurements. For the peak amplitude data there was found to be considerable scatter in the results with points ranging from 0.0002 to 10 m/s. Most of the high points (four of the six) were from Distant Zenith - although two of the Distant Zenith points were low and a point from both Mission Cyber and Disko Elm were just as high as the majority of points from Distant Zenith. There appears to be no real differences from one test to the other with regard to peak amplitude. The range observed in the roll off was from about -0.1 to -2.0 and there appears to be no change in the roll off as scaled range increases. There is one point from Distant Zenith that does not seem to fit the trend of the other measurements. This accelerometer was located 45 scaled meters from the source and the FFT from that gage is shown in Figure 3.13 along with the FFT of another ("normal") accelerometer that was located at 116 scaled meters. This is not one of the Distant Zenith gages that showed a late time of arrival of peak value (recall that those were all stress gages) but it is evident from the figure that the roll off is very much smaller than from the other gage.

The FFT analysis does not show any great differences among the results from any of the three events - either from the standpoint of stress measurements or accelerometer measurements.

4.0 Analysis of regional seismic signals

We examined the regional seismic data from the seismic networks operated by Lawrence Livermore National Laboratory (LLNL) and Sandia National Laboratory (SNL) in order to determine if any differences existed among the three tests were observed in the far field. The locations of the stations relative to the Nevada Test Site (NTS) are shown in Figure 4.1. The Livermore NTS Network (LNN) consists of four stations at distances ranging from approximately 180 to 400 km from NTS. Each station records two bands of data: a high-frequency band, flat to velocity between 1 and 30 Hz (GS-13 seismometer) and a broad-band channel, flat to velocity between 0.07 and 5 Hz (Sprengnether S-5100 seismometer); [Jarpe, 1989]. The SNL seismic network consists of five stations ranging at distances of approximately 144 to 379 km from NTS [Brady, 1989]. Sandia also transmits data in two different frequency bands each having a fairly narrow frequency response. For this study, we selected data from the short period band (Benioff seismometer) which was only available for Mission Cyber and Disko Elm.

Figure 4.2 shows seismograms overlaid for Mission Cyber and Disko Elm at the LLNL station KNB for the high-frequency and broad-band channels. Although the wave forms track quite well, it appears that Mission Cyber is slightly smaller than Disko Elm. Our approach to look at the relative coupling between the three tests was to take a number of measurements from the LLNL and

SNL regional seismic data from different phases (P_n, L_g, and coda) so that a statistically good determination could be made.

The measurements are illustrated in Figure 4.3. We manually measured a, b, and c values from the P_n phase and root-mean squared (RMS) values for the L_g phase (taken in a group velocity window of 3.6 to 3.0 km/s) and the seismogram coda (taken in a group velocity window of 3.0 to 1.5 km/s). For the RMS measurement, the signal was band-pass filtered between 0.75 and 1.25 Hz and the RMS value was computed using the formula

$$RMS = \sqrt{\frac{1}{N_s}\sum_{j=1}^{N_s} s_j^2 - \frac{1}{N_n}\sum_{j=1}^{N_n} n_j^2} \qquad (1)$$

where s_j is the j^{th} signal value in the measurement window, N_s is the number of signal values, n_j is the j^{th} noise value in a noise window taken 20 seconds prior to the P_n wave, and N_n is the number of noise values.

For each measurement we calculated a Δm_b value between each set of event pairs. In general, a seismic magnitude, m_b , is of the form

$$m_b = \log A + B(\Delta) \qquad (2)$$

where A is a seismic amplitude and $B(\Delta)$ is a distance correction. Seismic magnitudes are often observed to be linearly proportional to the explosion yield (cf. Vergino and Mensing, 1990), W , through the relationship

$$m_b = a \log W + b \qquad (3)$$

where a and b are the slope and intercept terms, respectively. Because of the close proximity of the explosions analyzed in this study the path to each of the stations is approximately the same so $B(\Delta)$ is approximately equal between the events and each station. Thus, when a Δm_b is calculated between explosion i and j we obtain from equations (2) and (3)

$$\Delta m_b = \log A_i - \log A_j = a(\log W_i - \log W_j) = a\,\Delta \log W \qquad (4)$$

giving

$$\Delta \log W = \frac{\Delta m_b}{a} \qquad (5)$$

The Δm_b values for different event pairs are listed in Table 4.1 and shown in Figure 4.4 for each station. From Figure 4.4 it can be seen that the Δm_b value is less than 1 for Mission Cyber / Disko Elm and Mission Cyber / Distant Zenith. From regional seismic data collected at the LLNL stations, the value of the slope, a, in equation (3) is observed to be approximately 0.9 for the P_n phase (Vergino and Mensing, 1990) and 0.8 for the Lg phase (Patton, 1988). Using an average value of 0.85 for the slope, we have listed the values for the corrected magnitudes. From equation (5), these values suggest that Mission Cyber is a factor of 0.75 that of Disko Elm and 0.65 that of Distant Zenith, and that Distant Zenith is a factor of 1.22 that of Disko Elm. To estimate the relative seismic coupling between the three events, it would be necessary to calculate the percentage difference between the yield ratio estimated from equation (5) and the actual ratio. Performing this calculation suggests that either Disko Elm coupled high and/or both Mission Cyber and Distant Zenith coupled low.

TABLE 4.1

Δm_b VALUES FOR NUCLEAR EXPLOSIONS USED IN THIS STUDY

RATIO	Δm_b	σ	N	Δm_b / 0.85
MISSION CYBER / DISKO ELM	-0.106	0.081	36	-0.124
DISTANT ZENITH / DISKO ELM	0.073	0.068	30	0.086
MISSION CYBER / DISTANT ZENITH	-0.161	0.112	20	-0.189

5.0 Conclusions

Data from the three tests conducted in P Tunnel have been analyzed from a number of different standpoints in an effort to determine if any basic differences exist with regard to the response of the tuff to the nuclear detonations. We have examined the quality of the rock, the response of close in stress and accelerometer gages, and the response of far field seismometers. We have compared the results from the P Tunnel tests with results from tests conducted in other tunnel testing.

Our examination of the core in P Tunnel indicated that the quality of rock at all three locations was strong and competent, at least out to a radius of 60 m from the working point. In fact, we believe the strength of the tuff in the vicinity of Mission Cyber working point was better than

would be indicated from looking at the results of static testing conducted by Terra Tek. In general, the core located away from the working points in a vertical direction was found to contain many layers of very weak, sandy-like material, some layers a few centimeters thick and some many meters thick. This layering characteristic should be incorporated in the constituent model for more accurate predictions of the ground motion at close-in as well as seismic distances. Even though these weak areas are well removed from the working point, they are still located close enough so that reflections could affect the outgoing pulse shapes. It is also felt that future testing should attempt to determine characteristics of this very weak unconsolidated material and its behavior under dynamic loading. The current rational for determining properties for use in the various predictive codes do not incorporate effects of these weaker layers because test samples cannot be fabricated due to the inherent weakness of the material.

Differences were found in the mineralogic content and the level of saturation of the tuff for the Mission Cyber test (compared to the other two test sites) and these differences could account for some of the scatter observed in the ground motion measurement records but would not result in great difference in behavior.

With regards to our examination of the close in stress and accelerometer gages there are several results that are puzzling. The arrival times of the peaks of the stress pulses from at least four, and as many as seven, of the stress gages from the Distant Zenith event could be interpreted as having late arrival times compared to the other Distant Zenith stress gages and stress gages from the other two tests. We could not correlate the identity of these gages with those that Sandia indicated could have been affected by the presence of known faults. The four gages with the largest delay were not singled out by Sandia as being of any significant problem. Of the other three stress gages which showed a smaller apparent time delay only two were identified by Sandia as being directly behind a known fault. Other gages that were identified by Sandia as being behind the fault actually had earlier times of arrival of peak stresses rather than later ones. In addition, Sandia had also identified accelerometers which were located behind a fault, but we found no abnormalities in the times of arrival (either peak arrival times or arrival times of first signal) in any of the accelerometers. It was also puzzling that the same stress gages that exhibited the late arrival time of the peak stress showed no abnormality in the arrival times of the first signal. Sandia indicated that the faults caused significantly reduced peak stress values. For some of the accelerometers records believed to be influenced by the fault, the peak values were four to five times higher than expected. The fact that faults would cause a decrease in the recorded stress values but an increase in the accelerations (and velocities and displacements) seems unconvincing. In the end, the argument that the presence of faults greatly alter the data from Distant Zenith was discarded and the variations were attributed to data scatter.

An examination of the magnitudes of stress, acceleration, velocity, and displacement

indicated that of the three tests there was less scatter in the Disko Elm data. The measurements from Disko Elm compare best with results obtained from testing in other tunnels. The most scatter appears in the data from Distant Zenith and the scatter is to both sides of the fit to the Disko Elm data. That is, some of the results from Distant Zenith are significantly higher than would be expected and some are significantly lower. There was very little scatter in the data from Mission Cyber and all of the data fall on the lower edge of the scatter from the Distant Zenith test. In general, the behavior of the tuff as determined from the average of all three P Tunnel tests is below the response determined in other tunnel testing.

Our examination of the rise times and pulse widths of the acceleration and stress records indicates that the behavior of Distant Zenith is in general different from the results of Mission Cyber and Disko Elm. Both the pulse widths and the rise times of the accelerometer records from Distant Zenith are significantly larger than from the other two events - but the rise times of the stress pulses from the Distant Zenith event are in agreement with similar rise times from the other two tests. This result appears to be contrary to our findings on apparent delay of arrival of peak values of the stress peaks. If the rise times are larger for the acceleration peaks than expected the arrival times of these peaks would be later, but they were not. If the rise times of the stress peaks was normal then it would be expected that the arrival times of those peaks would be normal, but they were later than expected.

There was good agreement among the rebound times among the three P Tunnel tests - both for the start of rebound and the end of rebound. Our examination did indicate that the total amount of time that movement back towards the source occurs appears to be considerably less (about 50%) for the P Tunnel tests than for Hunter's Trophy - an N Tunnel event. This should be investigated by examining the amount of displacement back towards the source in the P Tunnel tests compared to other tunnel testing. A smaller elastic rebound could help explain anomalies in the differences between dynamic and permanent displacements that occurred, especially in the Mission Cyber event.

From the standpoint of the shape of the stress pulse the "impulse" as determined from an integration of the stress versus time record appears to be greater for the Distant Zenith event than for the other two tests. Bear in mind that the results from such an integration should be viewed with some speculation since the stress does not return to zero because of residual stresses which made it necessary to select somewhat arbitrarily the upper limit on the time of integration.

The results of the seismic analysis indicated that Mission Cyber looks small compared to Disko Elm but also indicates that Distant Zenith looks smaller than it should compared to Disko Elm.

Our detailed analysis of the results from the P Tunnel tests has, therefore, lead us to the conclusion that there is no real reason to believe that the results obtained from the Mission Cyber

test are vastly different from the results obtained from the other two P Tunnel tests. The results from Mission Cyber fall within the scatter band which was determined from Distant Zenith and Disko Elm. Unlike Distant Zenith, all of the Mission Cyber points simply fall at the lower edge of the scatter band. Of the three tests Distant Zenith appeared to have the most scatter and Disko Elm the least.

Acknowledgments

Many people have contributed to our study. We acknowledge Carl Smith and Bob Bass at the Sandia National Laboratories for providing the ground motion and stress records from Mission Cyber, Disko Elm, and Distant Zenith and for taking time to discuss these shots with us. We thank Barbara Harris-West at the Defense Nuclear Agency at the Nevada Test Site for her assistance in arranging for us to examine the core, for collecting ground motion data for us, and helping us understand the tuff properties in P-Tunnel. The cooperation and expertise of Byron Ristvet at the Defense Nuclear Agency in Las Vegas, NV is very much appreciated. We appreciate Fred App's contribution in helping us interpret ground motion data from the tunnel tests. We appreciate the assistance of Jerry Magner, Mark Tsatsa, Ron Martin, Dick Hurlburt, and Harry Covington at the United States Geological Survey core library at the Nevada Test Site. We thank Susan Freeman for showing two of us (WLF and RDD) around Rainier and Pahute Mesas at the Nevada Test Site. We thank Doug Seastrand for providing SNL seismic data and Amanda Goldner and Keith Nakanishi for providing LLNL seismic data. We thank Eric Jones for reviewing the report. This work is performed under the auspices of the U.S. Department of Energy by Los Alamos National Laboratory under contract W-7405-ENG-36.

References

Bass, R.C., "Free-Field Ground Motion Induced by Underground Explosions", Sandia National Laboratory Report SAND74-0252, 1975.

Brady, L.F., "The Sandia Seismic Network," Sandia National Laboratory, Albuquerque, NM, EGG 10617, 11pp, 1989.

"Containment review of the DNA Mission Cyber Event (U)," Presented by DNA for presentation to the 166th CEP Meeting, 1987.

"Containment review of the DNA Disko Elm (U)," Presented by DNA for presentation to the 179th CEP Meeting, 1989.

"Containment review of the DNA Distant Zenith Event (U)," Presented by DNA for presentation to the CEP Meeting, 1991.

Fourney, W.L., R.D. Dick, and T.A. Weaver, "Explosive shielding by weak layers," Proceedings of the Numerical Modeling for Underground Nuclear Test Monitoring Symposium, Durango, CO, March 23-25, 1993, S.R. Taylor and J.R. Kamm, Eds., Los Alamos National Laboratory Report LA-UR-93-3839.

Jarpe, S.P., "Guide for using data from the LNN seismic monitoring network," Lawrence Livermore National Laboratory, Livermore, CA, UCID-21872, 5pp, 1989.

Patton, H.J., "Application of Nuttli's method to estimate yield of Nevada Test Site explosions recorded on Lawrence Livermore National Laboratory's Digital Seismic System," Bull. Seis. Soc. Am. 78, 1759-1772, 1988.

Torres, G. "Characterization of material from the Nevada Test Site, final report for the period January 1986 through March 1988 - Volumes I,II, III," DNA-TR-88-278-V1, V2, V3,1988.

Vergino, E.S. and R.W. Mensing, "Yield estimation using regional $m_b(P_n)$," Bull. Seis. Soc. Am., 80, 656-674, 1990.

FIGURE CAPTIONS

Figure 1.1 Tunnel Level Map of Mission Cyber (U12P.02), Disko Elm (U12P.03), and Distant Zenith (U12P.04) and the Location of the Exploratory Core Holes.

Figure 1.2 Stratigraphic Section and the Event Level at Which the Three Tests Were Conducted.

Figure 1.3 Disko Elm Exploratory Horizontal Holes and SNL Instrument Holes Typical for These Test Locations.

Figure 2.1 Relative Strength Versus Depth for the Vertical Core Hole UE12P.04 Near Mission Cyber.

Figure 2.2 Relative Strength Versus Depth for the Vertical Core Hole UE12P.04 Calibrated from Terra Tek Strength Data.

Figure 2.3 Relative Strength Versus Length for U12P IH-1.

Figure 2.4 Relative Strength Versus Length for U12P.06 UG-1.

Figure 3.1a Typical Stress Measurements From Mission Cyber Event.

Figure 3.1b Typical Stress Measurements From Disko Elm Event.

Figure 3.1c Typical Stress Measurements From Distant Zenith Event.

Figure 3.2a Typical Acceleration Measurements From Mission Cyber Event.

Figure 3.2b Typical Acceleration Measurements From Disko Elm Event.

Figure 3.2c Typical Acceleration Measurements From Distant Zenith Event.

Figure 3.3 Time of Arrival Versus Scaled Range for Peak Stress Values From DZ Compared to Least Square Fit of DE and MC Data.

Figure 3.4 Stress Measurements From Three P Tunnel Events Compared to Expected Results. 1 - Distant Zenith, 2 - Mission Cyber, 3 - Disko Elm.

Figure 3.5 Acceleration Levels Measured in P Tunnel Events Compared to Expected Results 1 - Distant Zenith, 2 - Mission Cyber, 3 - Disko Elm.

Figure 3.6 Velocities Measured in P Tunnel Events Compared to Expected Results. 1 - Distant Zenith, 2 - Mission Cyber, 3 - Disko Elm.

Figure 3.7 Dynamic Peak Displacements From DE and MC Compared to Permanent Displacements From MC.

Figure 3.8 Acceleration Pulse Width Comparison of Results From Three P Tunnel Events - Lines are Least Square Fits. 1 - Distant Zenith, 2 - Mission Cyber, 3 - Disko Elm.

Figure 3.9 Acceleration Risetime Comparison of Results From Three P Tunnel Events. 1 - Distant Zenith, 2 - Mission Cyber, 3 - Disko Elm.

Figure 3.10 Typical Velocity Trace Showing Two Rebound Times - RB1 and RB2.

Figure 3.11a Rebound Time RB1 From Three P Tunnel Events and From Hunter's Trophy.

Figure 3.11b Time Duration of Velocity Towards Source (RB2-RB1) From Three P Tunnel Events and For Hunter's Trophy.

Figure 3.12 Comparison of "Impulse" (Area Under Stress Time Curve) From Three P Tunnel Tests - Lines are Least Square Fits. 1 - Distant Zenith, 2 - Mission Cyber, 3 - Disko Elm.

Figure 3.13 Frequency Spectra From Two Accelerometers From Distant Zenith Showing Large Difference in Roll Off.

Figure 4.1. Location of seismic stations of the Livermore NTS Network (LNN; open triangles) and the Sandia Seismic Network (open circles).

Figure 4.2. Vertical-component seismograms at LLNL station KNB (Kanab, UT) for Disko Elm (solid line) and Mission Cyber (dashed line) on the high-frequency channel and the broad-band channel (high-pass filtered at 0.5 Hz).

Figure 4.3. Examples of measurements on the high-frequency vertical-component seismogram at KNB. Top portion of the figure shows measurements used to calculate a, b, and c values from the P_n wave (a = T1 - 0; b = | T1 - T2 |; c = | T3 - T2|). The bottom portion of the figure shows the windows used for the Lg RMS (T4 to T5) and coda RMS (T5 to T6) calculations (band-pass filtered between 0.75 and 1.25 Hz).

Figure 4.4. Δm_b values and 2σ errors for different measurements and event pairs. (a) Mission Cyber / Disko Elm; (b) Distant Zenith / Disko Elm; and (c) Mission Cyber / Distant Zenith. Station indicators (see Figure S1): B - BTM; D - DRW; L - LDS; N - NLS; T - TON; EH - ELK HF; KH - KNB HF; LH - LAC HF; MH - MNV HF; EB - ELK BB; KB - KNB BB; LB - LAC BB; MB - MNV BB.

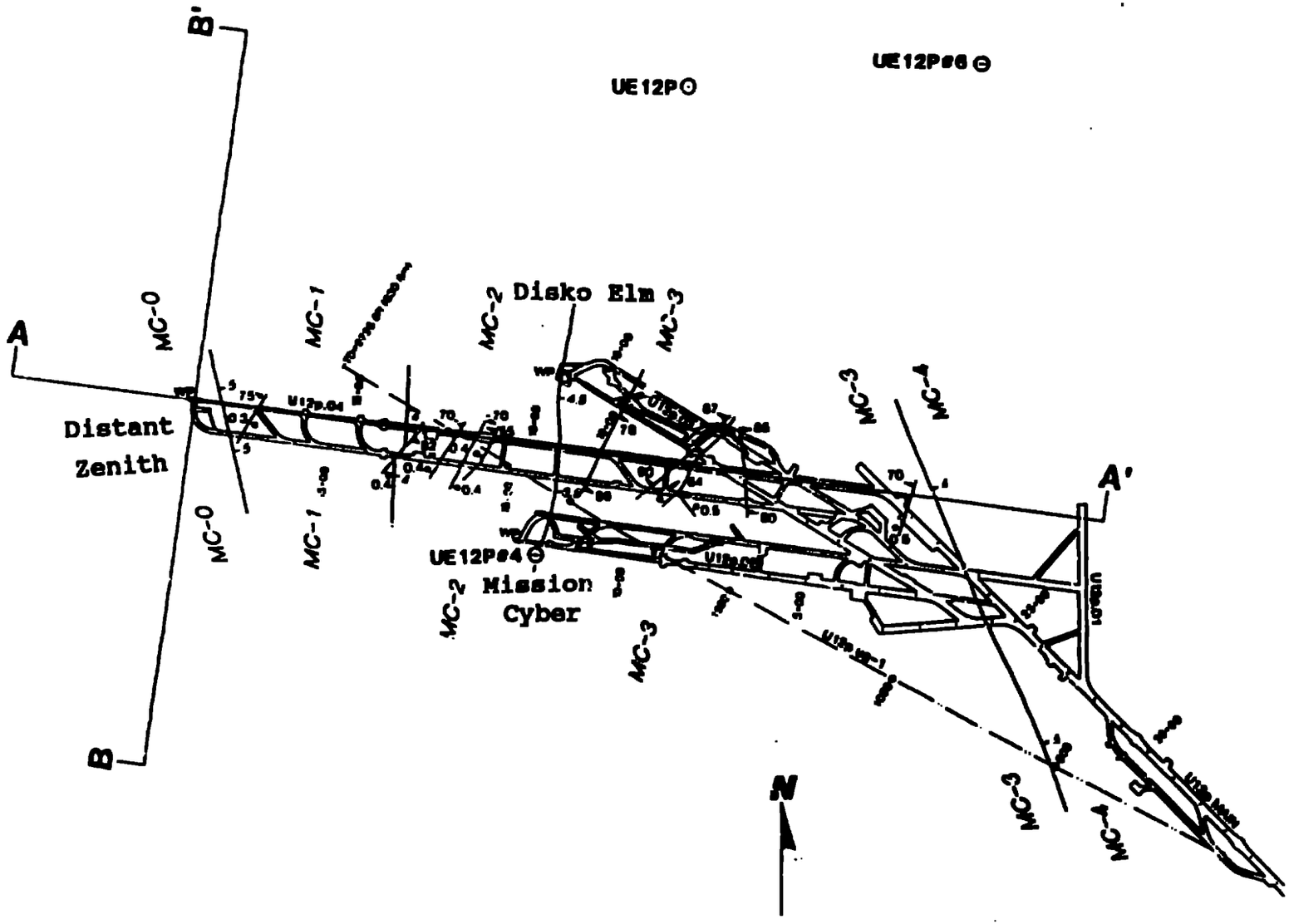
B'
UE12P⊙
UE12Ps6 ⊖
A
MC-0
MC-1
MC-2
Disko Elm
MC-3
MC-4
Distant
Zenith
A'
B
UE12Ps4 ⊖
Mission
Cyber
N
MC-0
MC-1
SUBUNIT CONTACT –bedding dip direction and magnitude as indicated
FAULT–bar and ball on downthrown side Displacement in meters.
FRACTURE–dip direction and magnitude as indicated
UE12P⊙ VERTICAL
0 100 200 feet

Figure 1.1

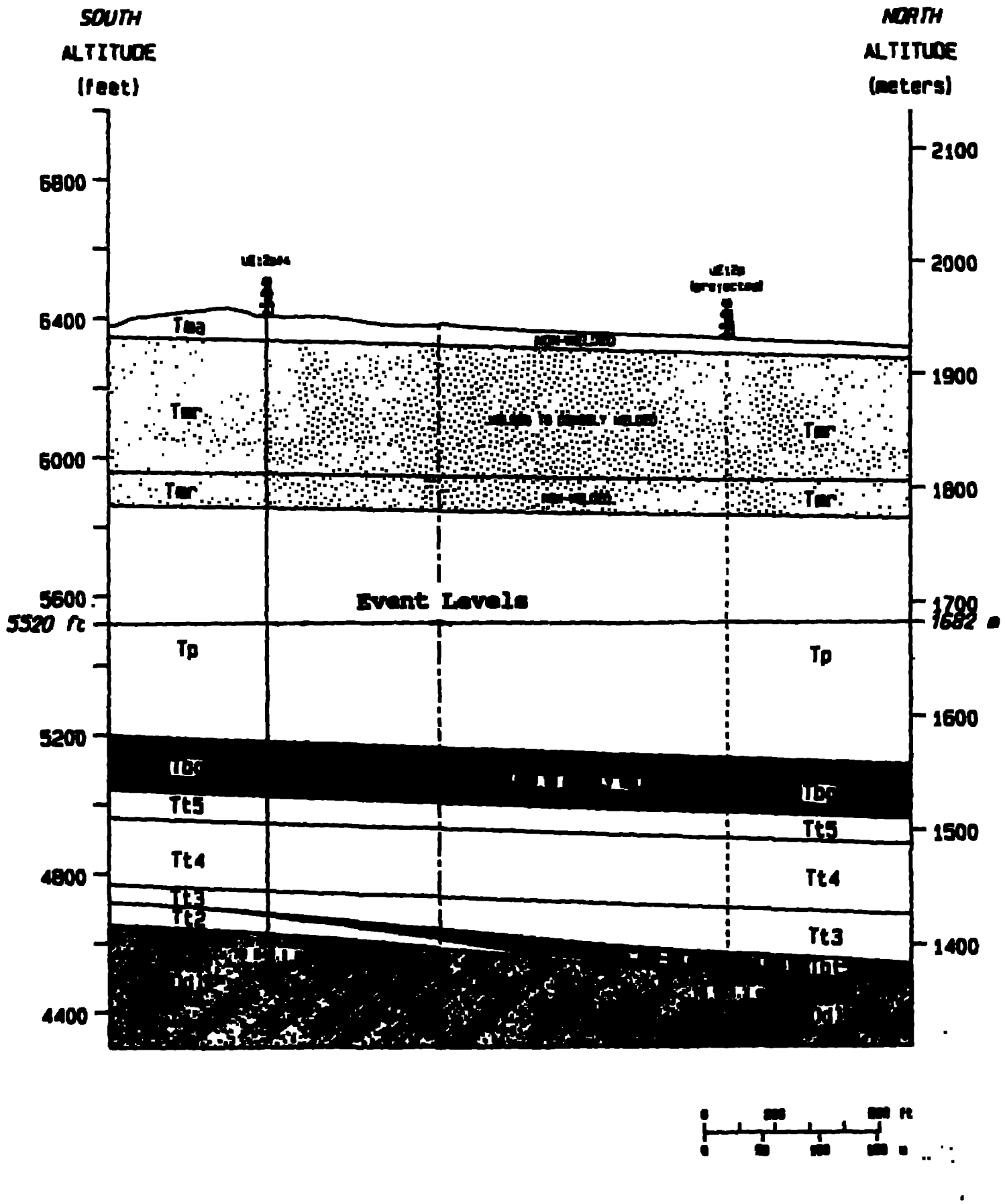
SOUTH
ALTITUDE
(feet)
NORTH
ALTITUDE
(meters)
6800
6400
6000
5600
5520 ft
5200
4800
4400
2100
2000
1900
1800
1700
1682 m
1600
1500
1400
Tma
Tmr
Tmr
Tmr
Tmr
Event Levels
Tp
Tp
Tt5
Tt5
Tt4
Tt4
Tt3
Tt3

DRILL HOLE DESCRIPTION

HOLE NUMBER	HOLE DIAMETER	TOTAL DEPTH	HOLE NUMBER	HOLE DIAMETER	TOTAL DEPTH
1. CH#3	152.4MM	23.3M	22. SR#7	76MM	19.6M
2. CH#4	101.6MM	23M	23. SR#8	76MM	16M
3. CH#5	101.6MM	25M	24. RGH#1A	76MM	1.8M
4. CH#6	101.6MM	25.3M	25. RGH#2A	76MM	1.8M
5. GI#1	75.7MM	42.6M	26. RGH#3A	76MM	1.8M
6. IH#1	203MM	99M	27. RGH#4A	76MM	1.8M
7. IH#2	203MM	78M	28. RGH#5A	76MM	1.8M
8. IH#3	203MM	127M	29. RGH#6A	76MM	1.8M
9. IH#4	203MM	36.5M	30. RGH#7A	76MM	2M
10. IH#5	203MM	36.5M	31. RGH#1B	76MM	1.8M
11. IH#6	101.6MM	9.7M	32. RGH#2B	76MM	2M
12. IH#7	101.6MM	6.6M	33. RGH#3B	76MM	1.8M
13. IH#8	203MM	34.7M	34. IH#13	305MM	3M
14. IH#11	609.6MM	6M	35. GI#2	76MM	137M
15. IH#12	203MM	25.6M	36. PS-1	76MM	6M
16. SR#1	76MM	19.4M	37. PS-2	76MM	9M
17. SR#2	76MM	20.4M	38. PS-3	76MM	6M
18. SR#3	76MM	19.7M	39. PS-4	76MM	9M
19. SR#4	76MM	16M	40. PS-5	76MM	6M
20. SR#5	76MM	18.5M	41. PS-6	76MM	9M
21. SR#6	76MM	20.3M	42. PS-7	76MM	6M
			43. PS-8	76MM	9M

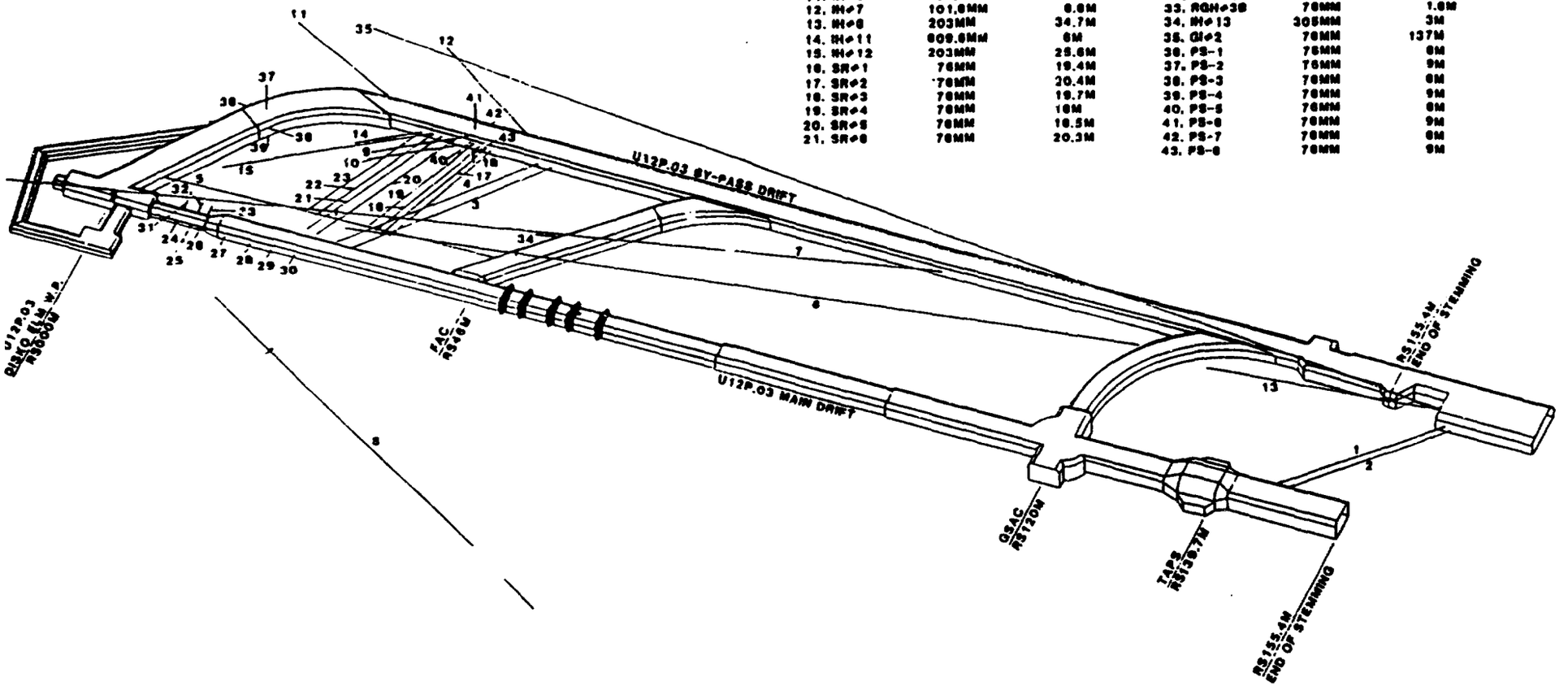

Figure 1.3

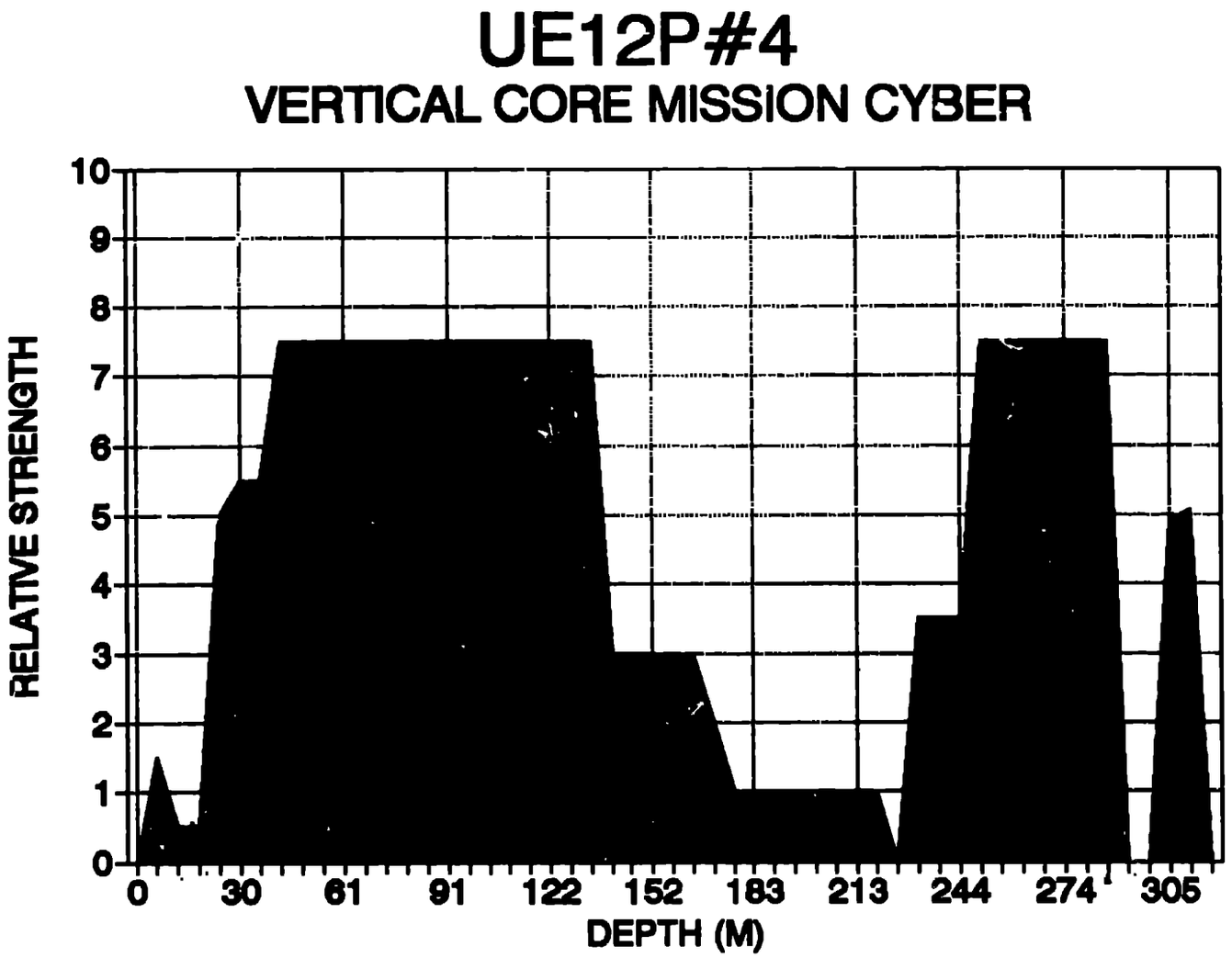
UE12P#4
VERTICAL CORE MISSION CYBER
RELATIVE STRENGTH
10
9
8
7
6
5
4
3
2
1
0
0
30
61
91
122
152
183
213
244
274
305
DEPTH (M)

Figure 2.1

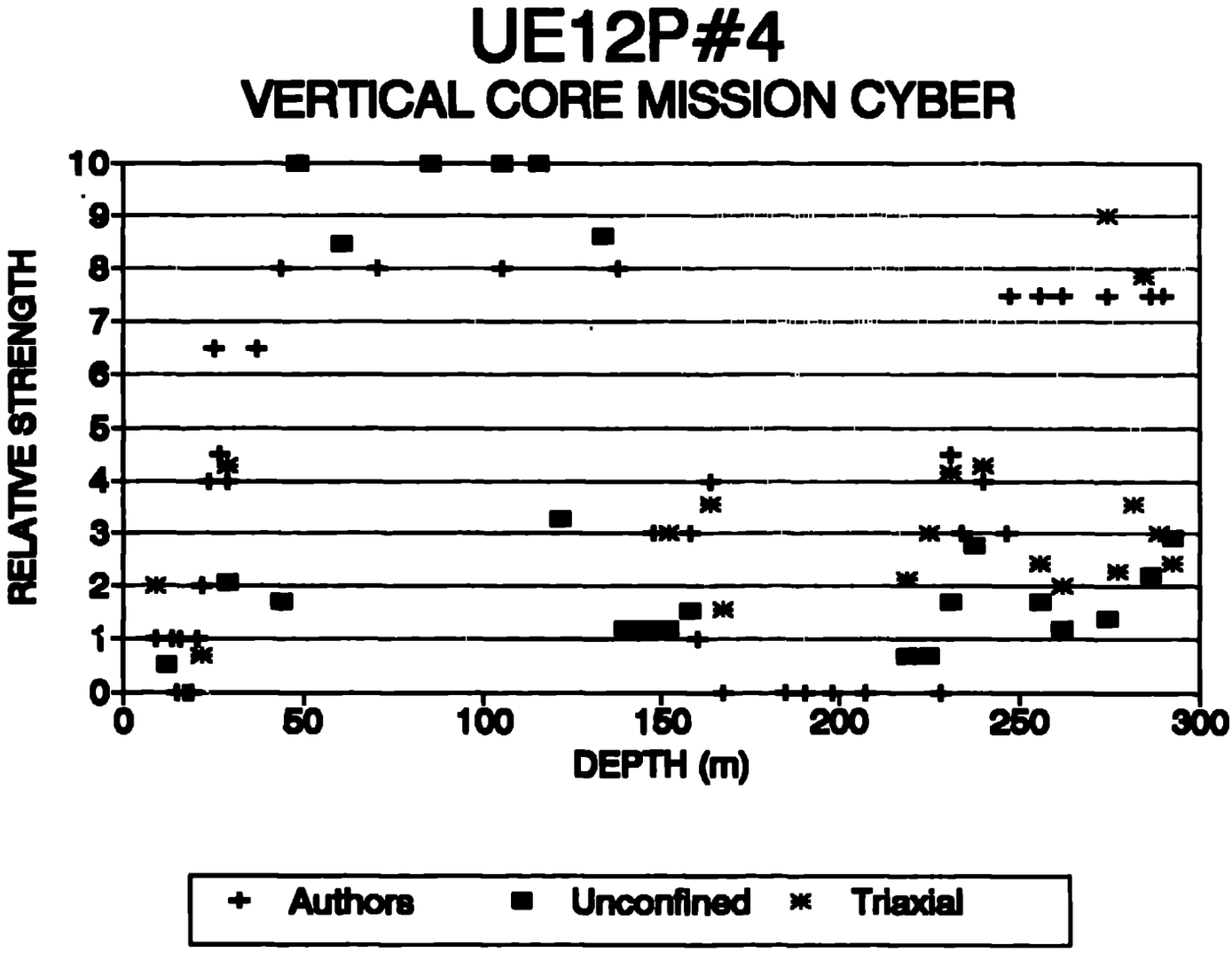
UE12P#4
VERTICAL CORE MISSION CYBER
RELATIVE STRENGTH
10
9
8
7
6
5
4
3
2
1
0
0
50
100
150
200
250
300
DEPTH (m)
Authors
Unconfined
Triaxial

Figure 2.2

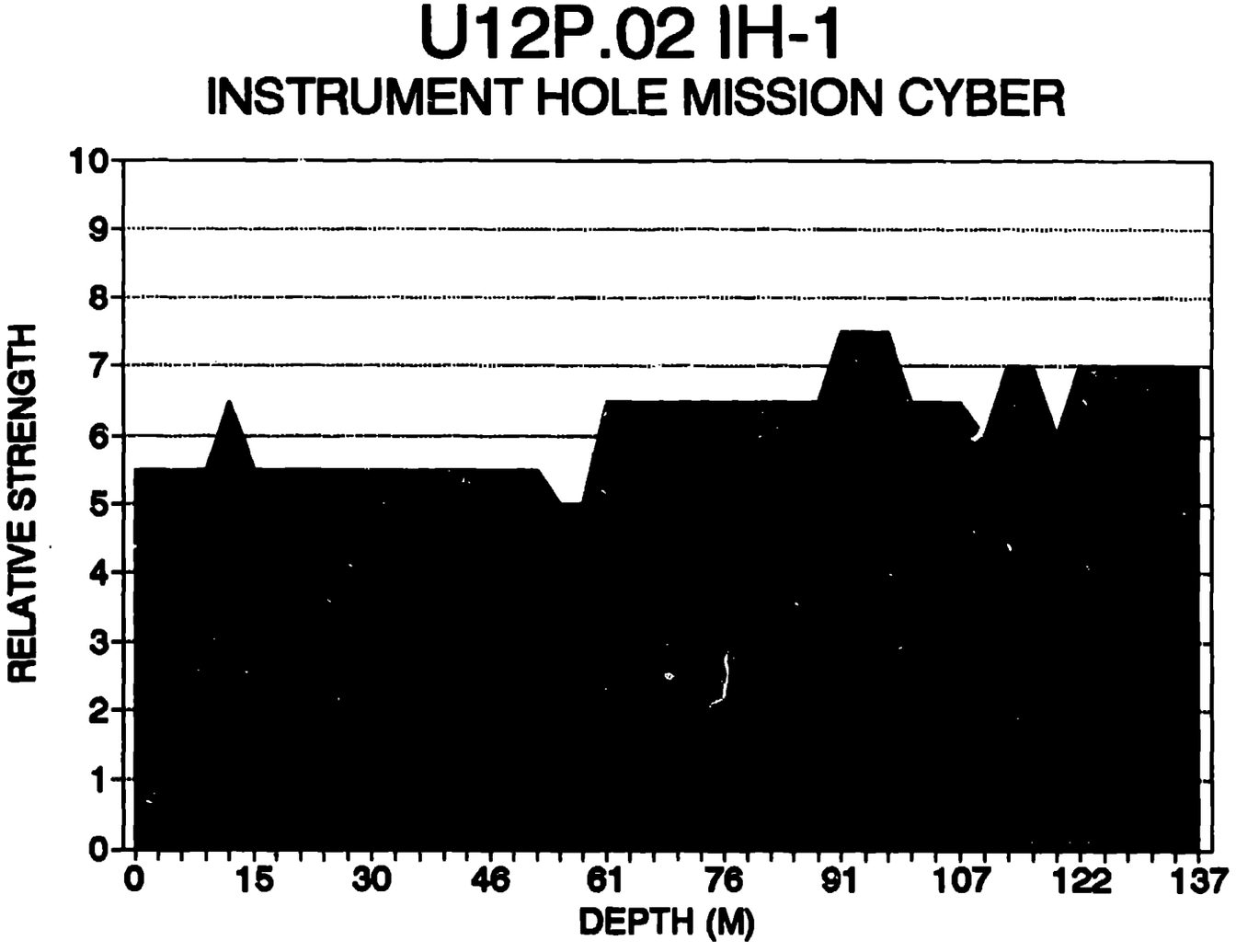
U12P.02 IH-1
INSTRUMENT HOLE MISSION CYBER
RELATIVE STRENGTH
10
9
8
7
6
5
4
3
2
1
0
0
15
30
46
61
76
91
107
122
137
DEPTH (M)

Figure 2.3

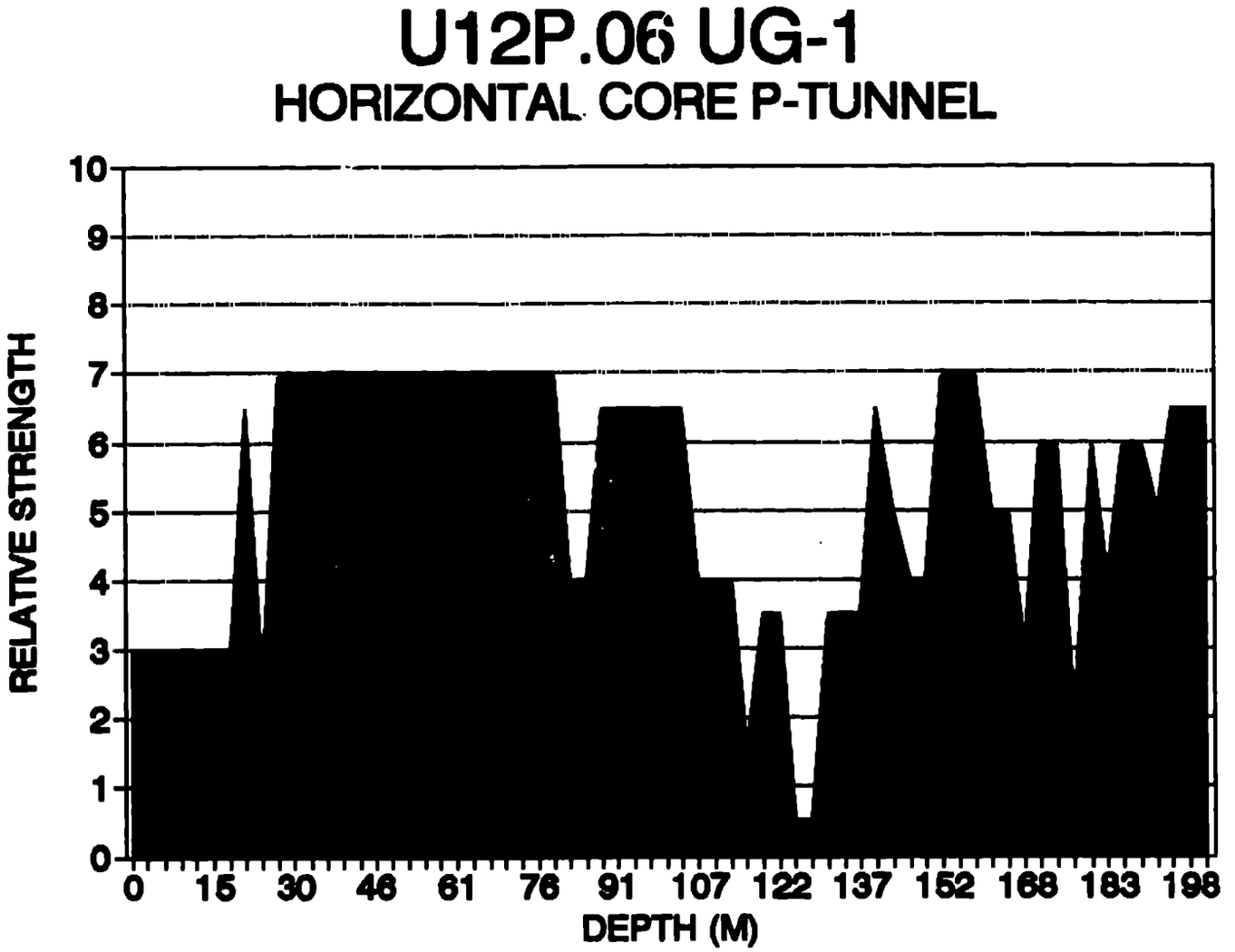
U12P.06 UG-1
HORIZONTAL CORE P-TUNNEL
RELATIVE STRENGTH
10
9
8
7
6
5
4
3
2
1
0
0 15 30 46 61 76 91 107 122 137 152 168 183 198
DEPTH (M)

Figure 2.4

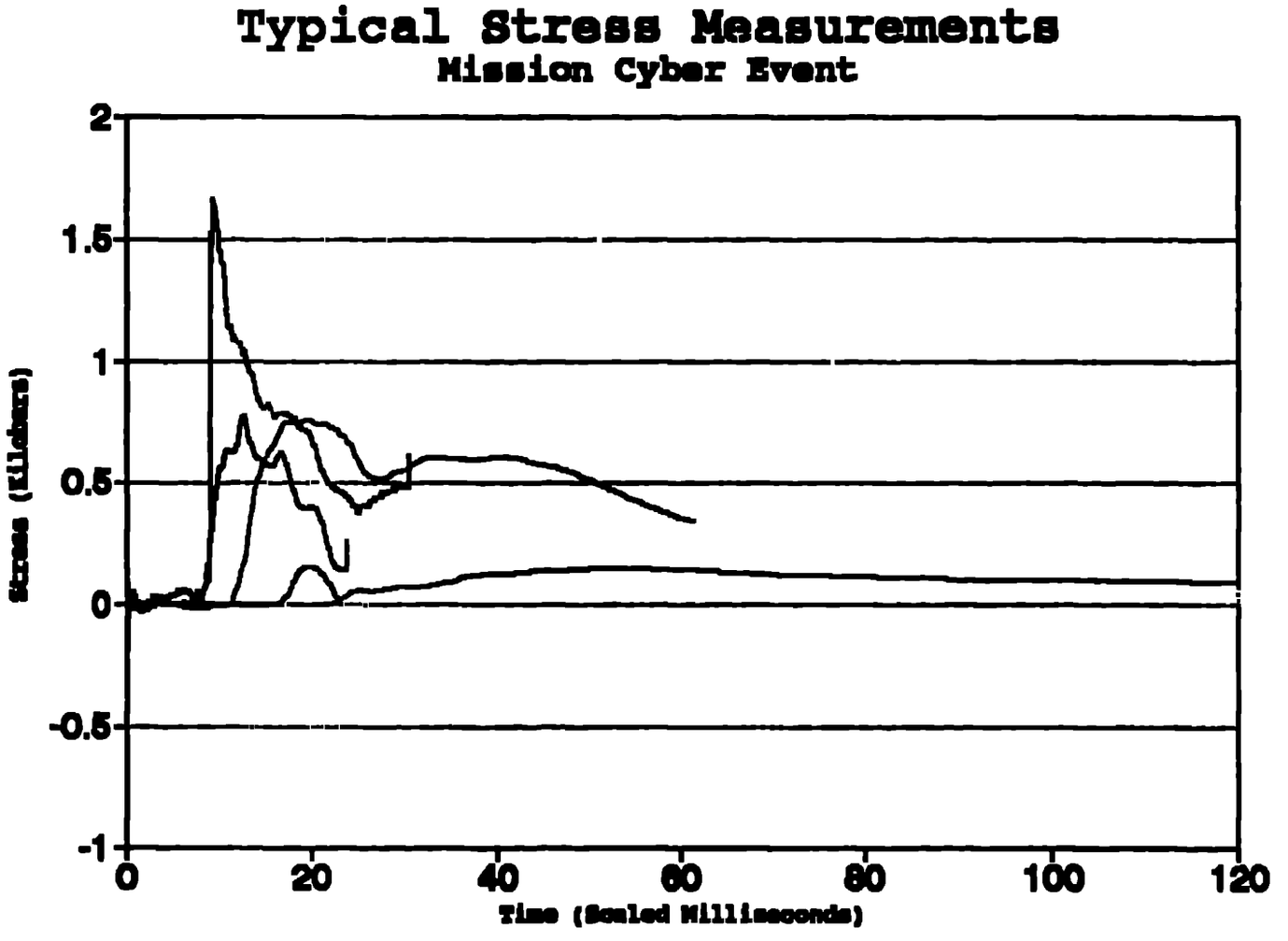
Typical Stress Measurements
Mission Cyber Event
Stress (Kilobars)
2
1.5
1
0.5
0
-0.5
-1
0
20
40
60
80
100
120
Time (Scaled Milliseconds)

Figure 3.1a

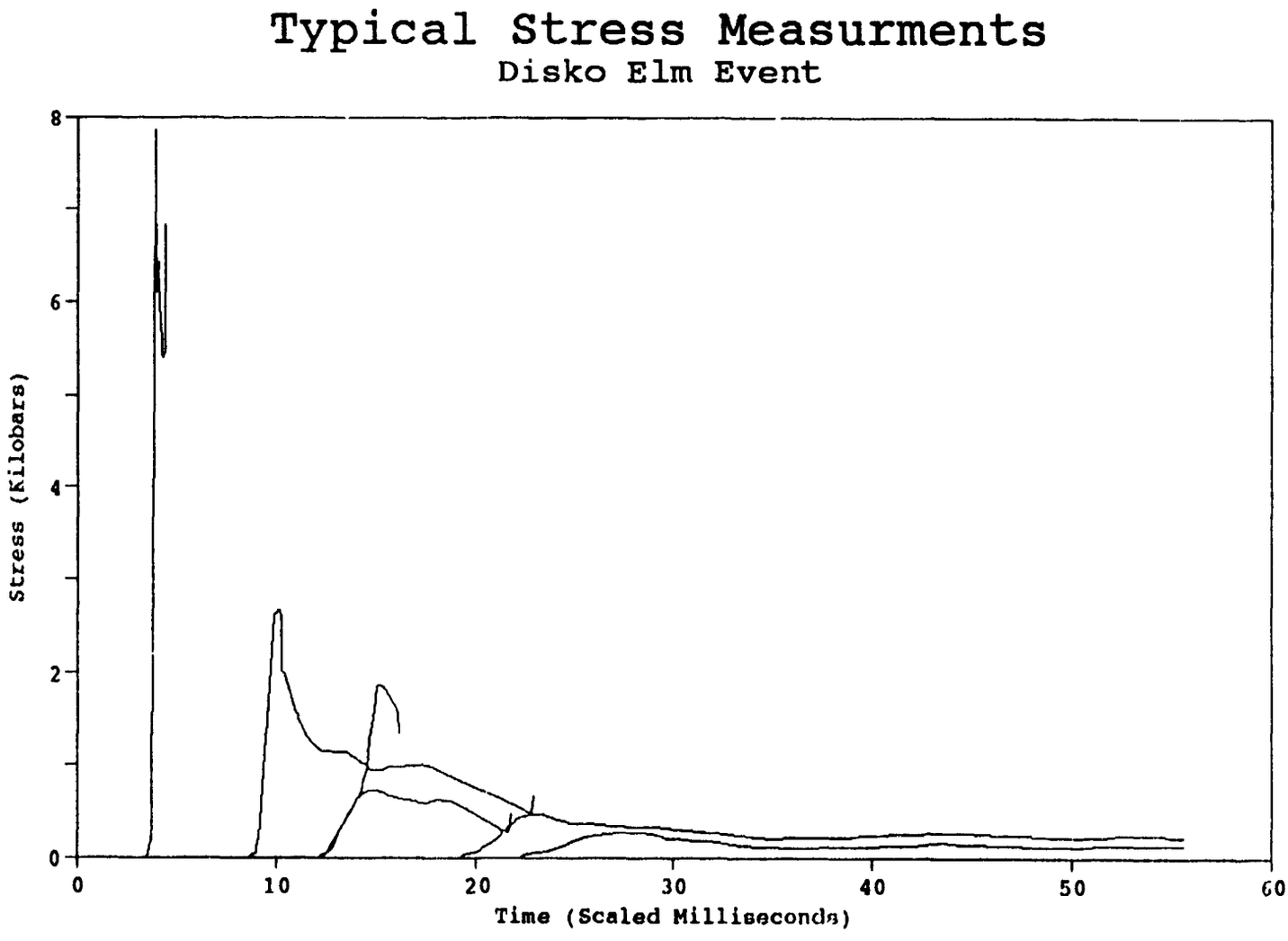
Typical Stress Measurments
Disko Elm Event
Stress (Kilobars)
8
6
4
2
0
0
10
20
30
40
50
60
Time (Scaled Milliseconds)

Figure 3.1b

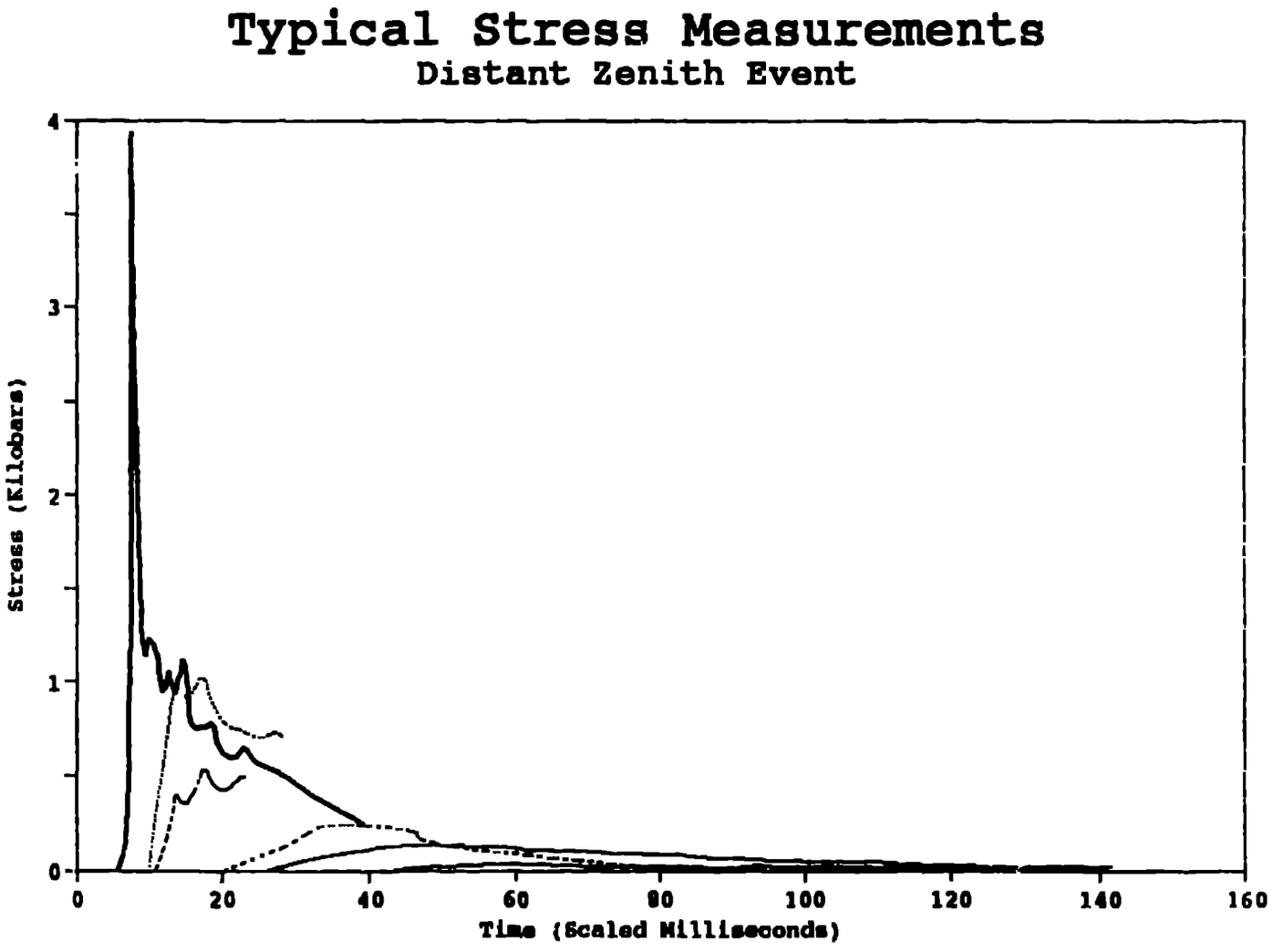
Typical Stress Measurements
Distant Zenith Event
Stress (Kilobars)
Time (Scaled Milliseconds)
0
1
2
3
4
0
20
40
60
80
100
120
140
160

Figure 3.1c

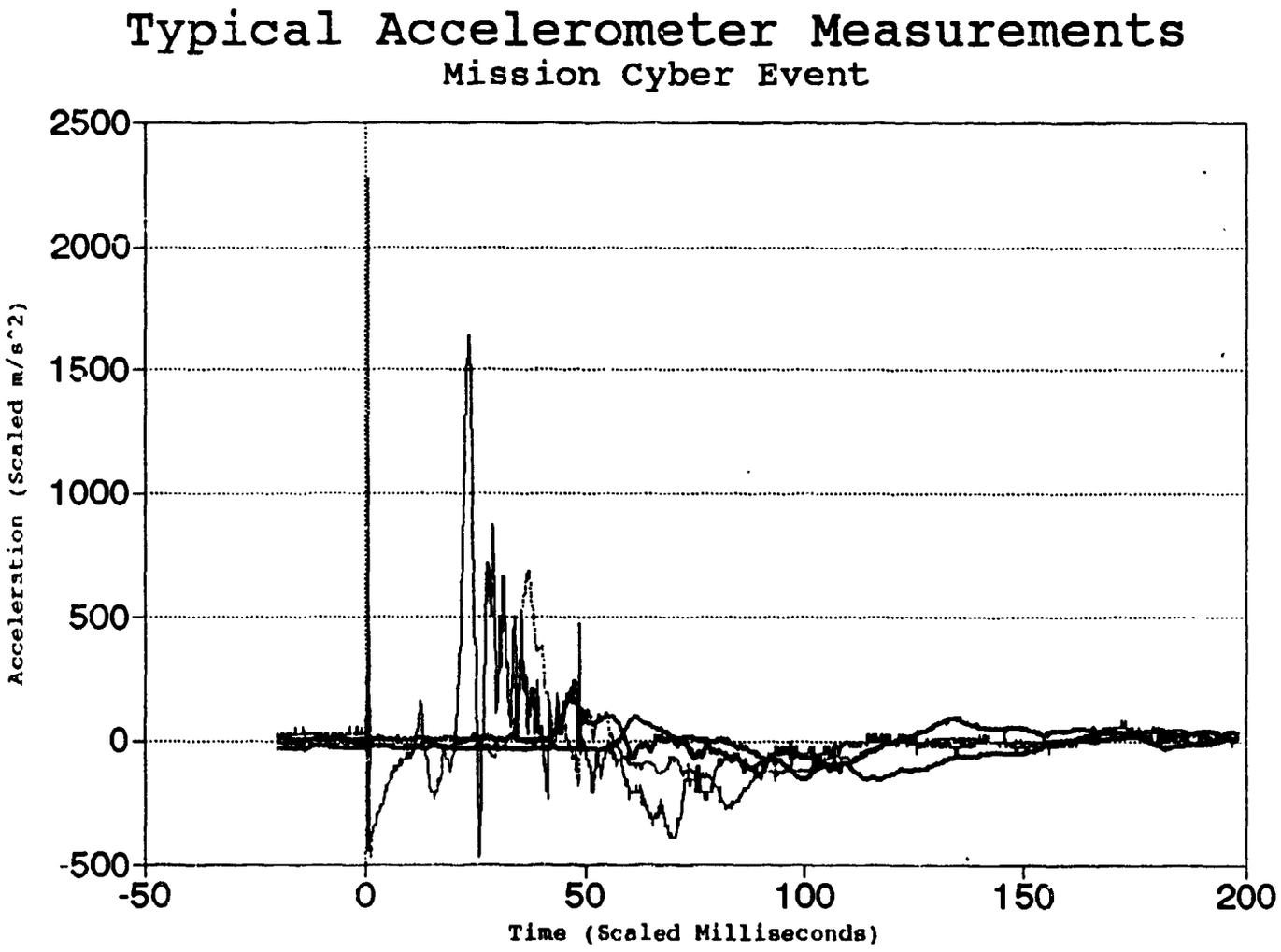
Typical Accelerometer Measurements
Mission Cyber Event
Acceleration (Scaled m/s^2)
2500
2000
1500
1000
500
0
-500
-50
0
50
100
150
200
Time (Scaled Milliseconds)

Figure 3.2a

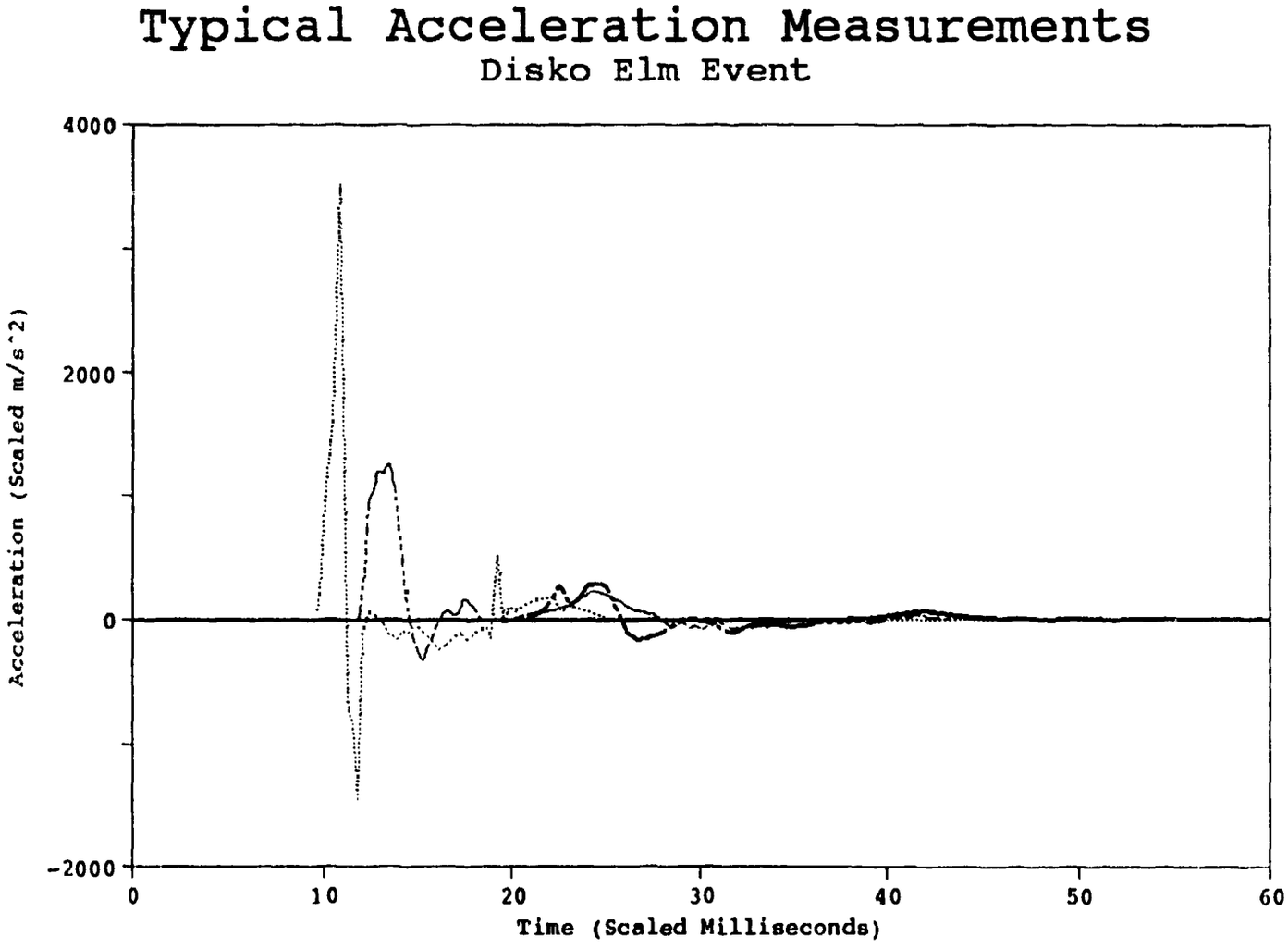
Typical Acceleration Measurements
Disko Elm Event
4000
2000
0
-2000
Acceleration (Scaled m/s^2)
0
10
20
30
40
50
60
Time (Scaled Milliseconds)

Figure 3.2b

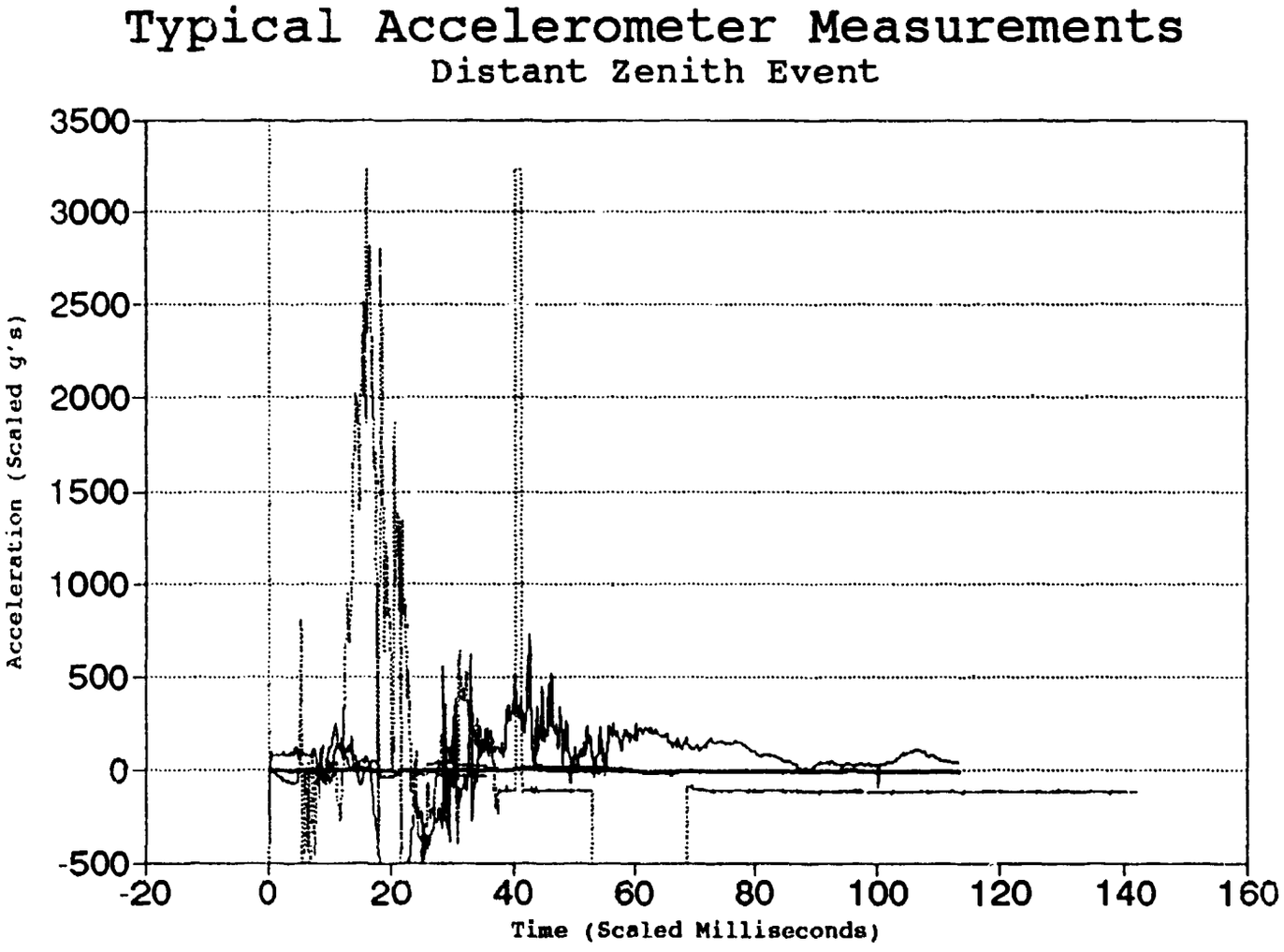
Typical Accelerometer Measurements
Distant Zenith Event
Acceleration (Scaled g's)
3500
3000
2500
2000
1500
1000
500
0
-500
-20
0
20
40
60
80
100
120
140
160
Time (Scaled Milliseconds)

Figure 3.2c

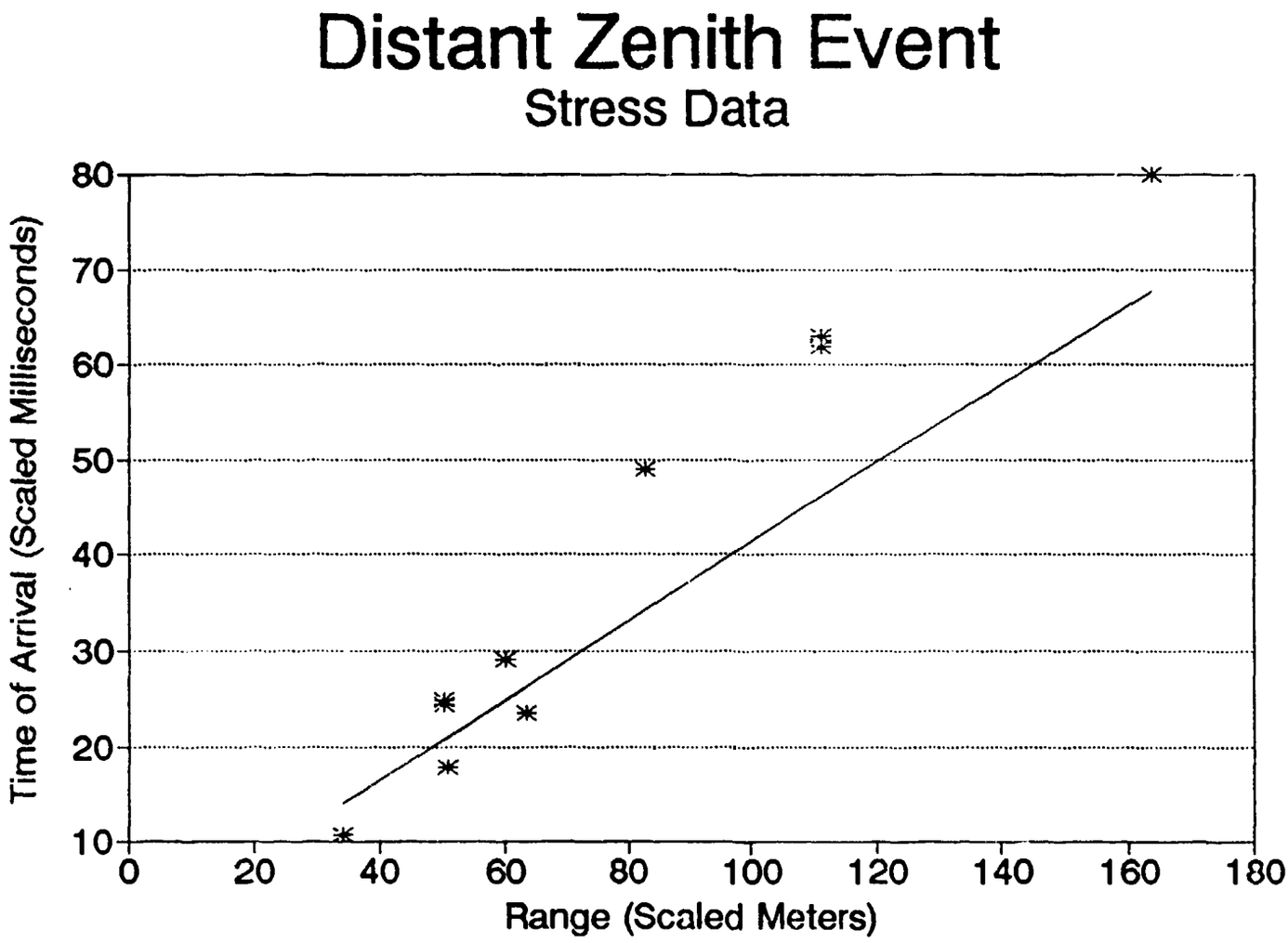
Distant Zenith Event
Stress Data
Time of Arrival (Scaled Milliseconds)
80
70
60
50
40
30
20
10
0
20
40
60
80
100
120
140
160
180
Range (Scaled Meters)

Figure 3.3

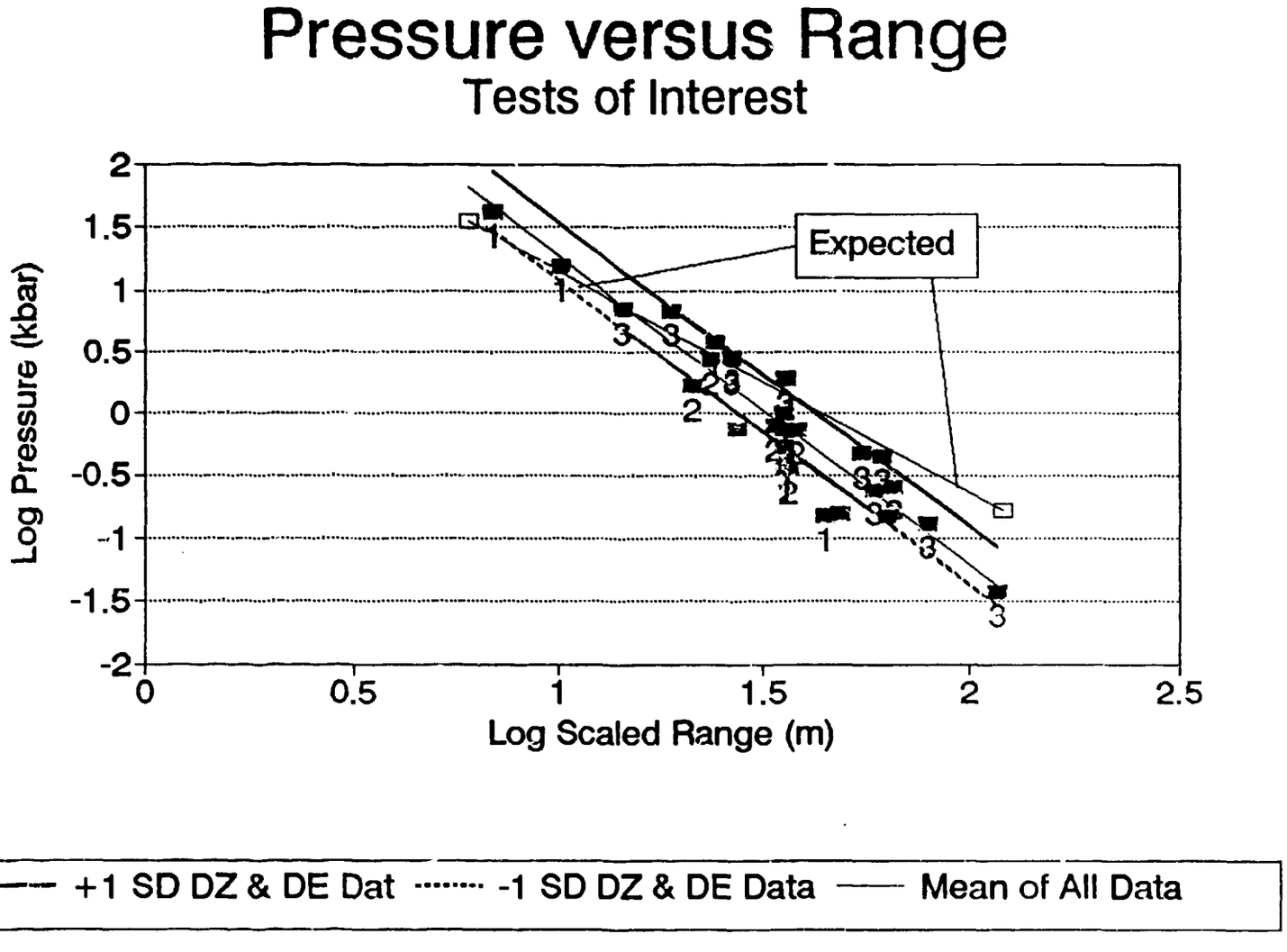
Pressure versus Range
Tests of Interest
Log Pressure (kbar)
2
1.5
1
0.5
0
-0.5
-1
-1.5
-2
0
0.5
1
1.5
2
2.5
Log Scaled Range (m)
Expected
+1 SD DZ & DE Dat
-1 SD DZ & DE Data
Mean of All Data

Figure 3.4

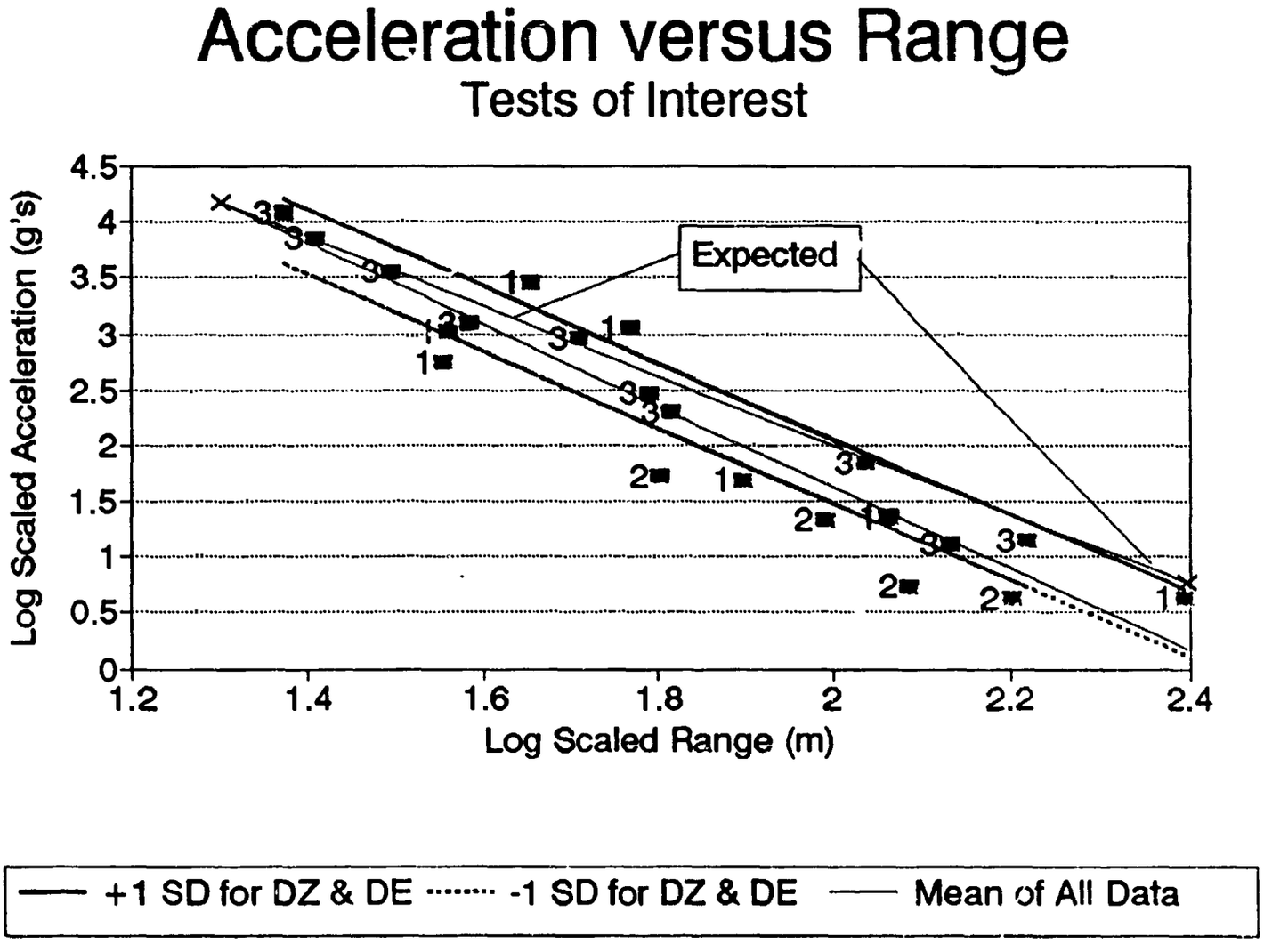
Acceleration versus Range
Tests of Interest
Log Scaled Acceleration (g's)
Log Scaled Range (m)
Expected
4.5
4
3.5
3
2.5
2
1.5
1
0.5
0
1.2
1.4
1.6
1.8
2
2.2
2.4
+1 SD for DZ & DE
-1 SD for DZ & DE
Mean of All Data

Figure 3.5

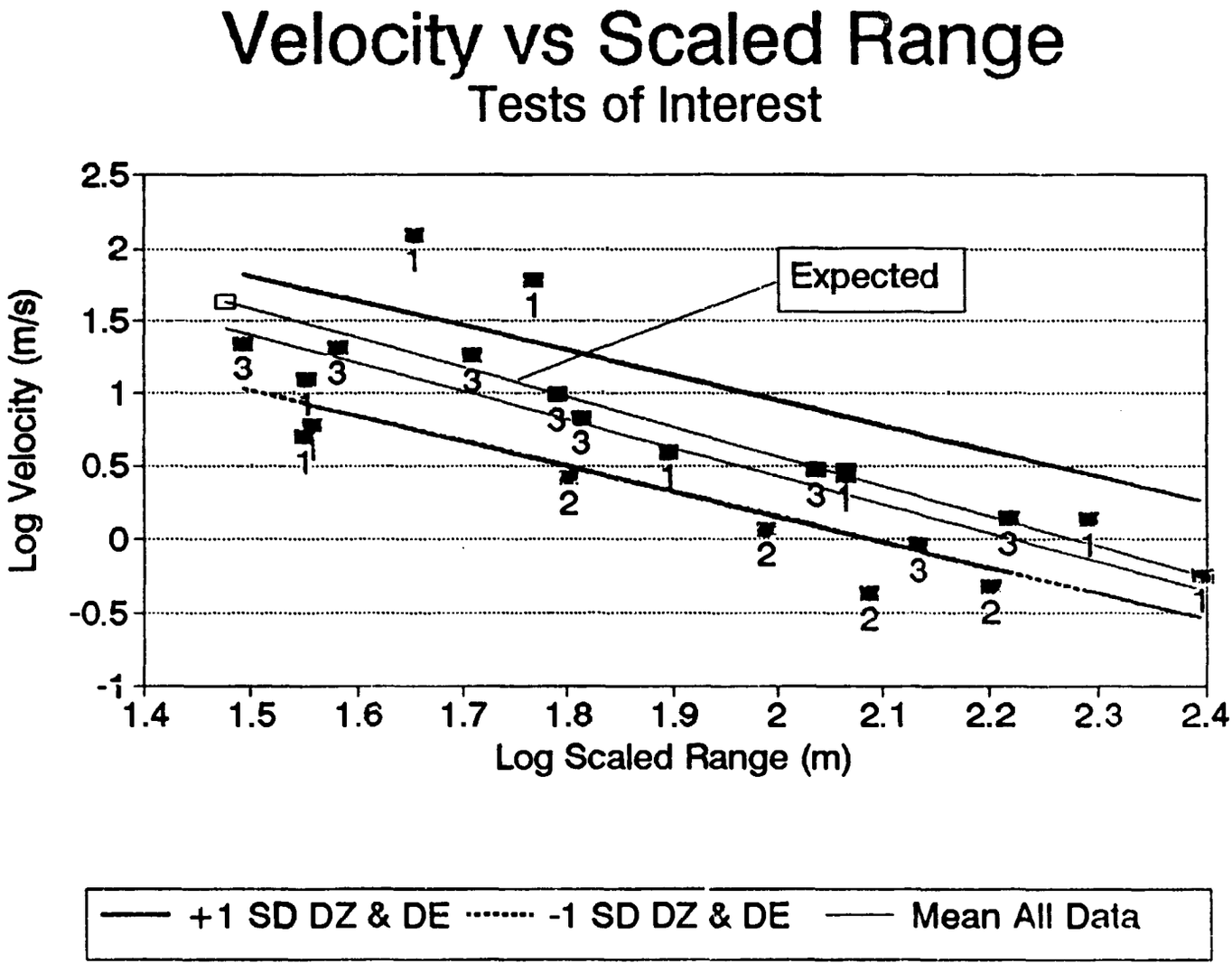
Velocity vs Scaled Range
Tests of Interest
Log Velocity (m/s)
2.5
2
1.5
1
0.5
0
-0.5
-1
1.4
1.5
1.6
1.7
1.8
1.9
2
2.1
2.2
2.3
2.4
Log Scaled Range (m)
Expected
+1 SD DZ & DE
-1 SD DZ & DE
Mean All Data

Figure 3.6

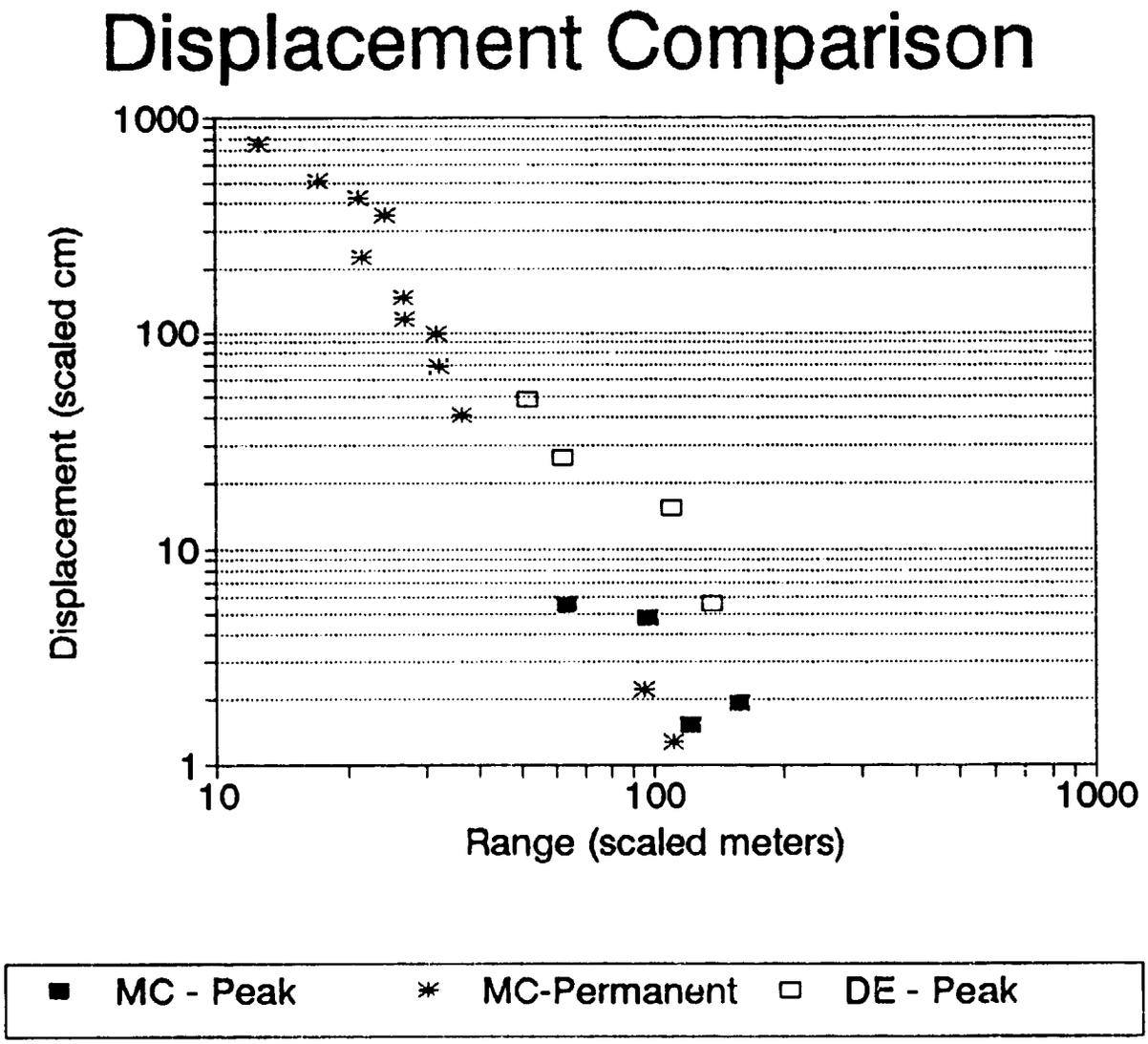
Displacement Comparison
1000
100
10
1
Displacement (scaled cm)
10
100
1000
Range (scaled meters)
MC - Peak
MC-Permanent
DE - Peak

Figure 3.7

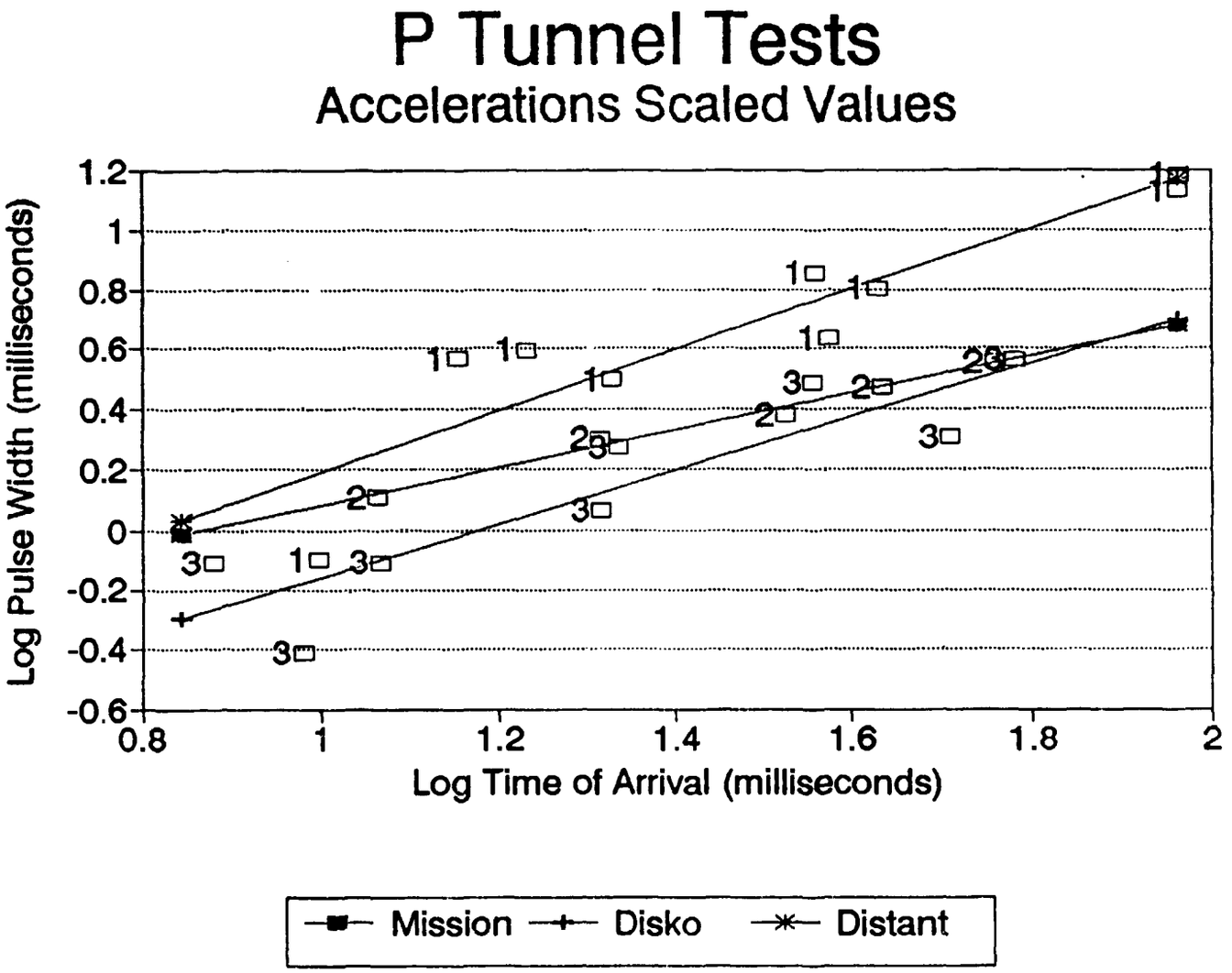
P Tunnel Tests
Accelerations Scaled Values
Log Pulse Width (milliseconds)
1.2
1
0.8
0.6
0.4
0.2
0
-0.2
-0.4
-0.6
0.8
1
1.2
1.4
1.6
1.8
2
Log Time of Arrival (milliseconds)
Mission
Disko
Distant

Figure 3.8

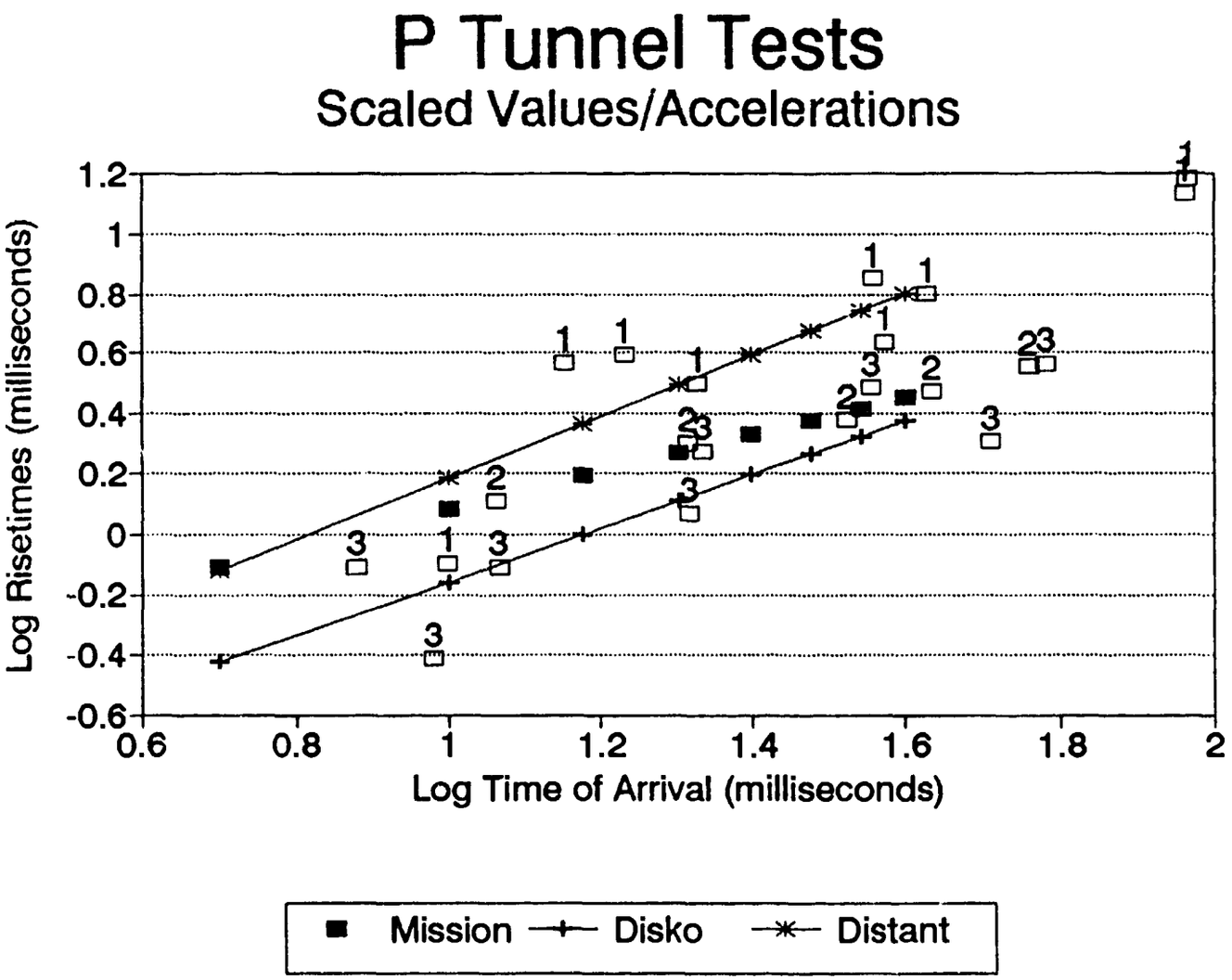
P Tunnel Tests
Scaled Values/Accelerations
Log Risetimes (milliseconds)
1.2
1
0.8
0.6
0.4
0.2
0
-0.2
-0.4
-0.6
0.6
0.8
1
1.2
1.4
1.6
1.8
2
Log Time of Arrival (milliseconds)
Mission
Disko
Distant

Figure 3.9

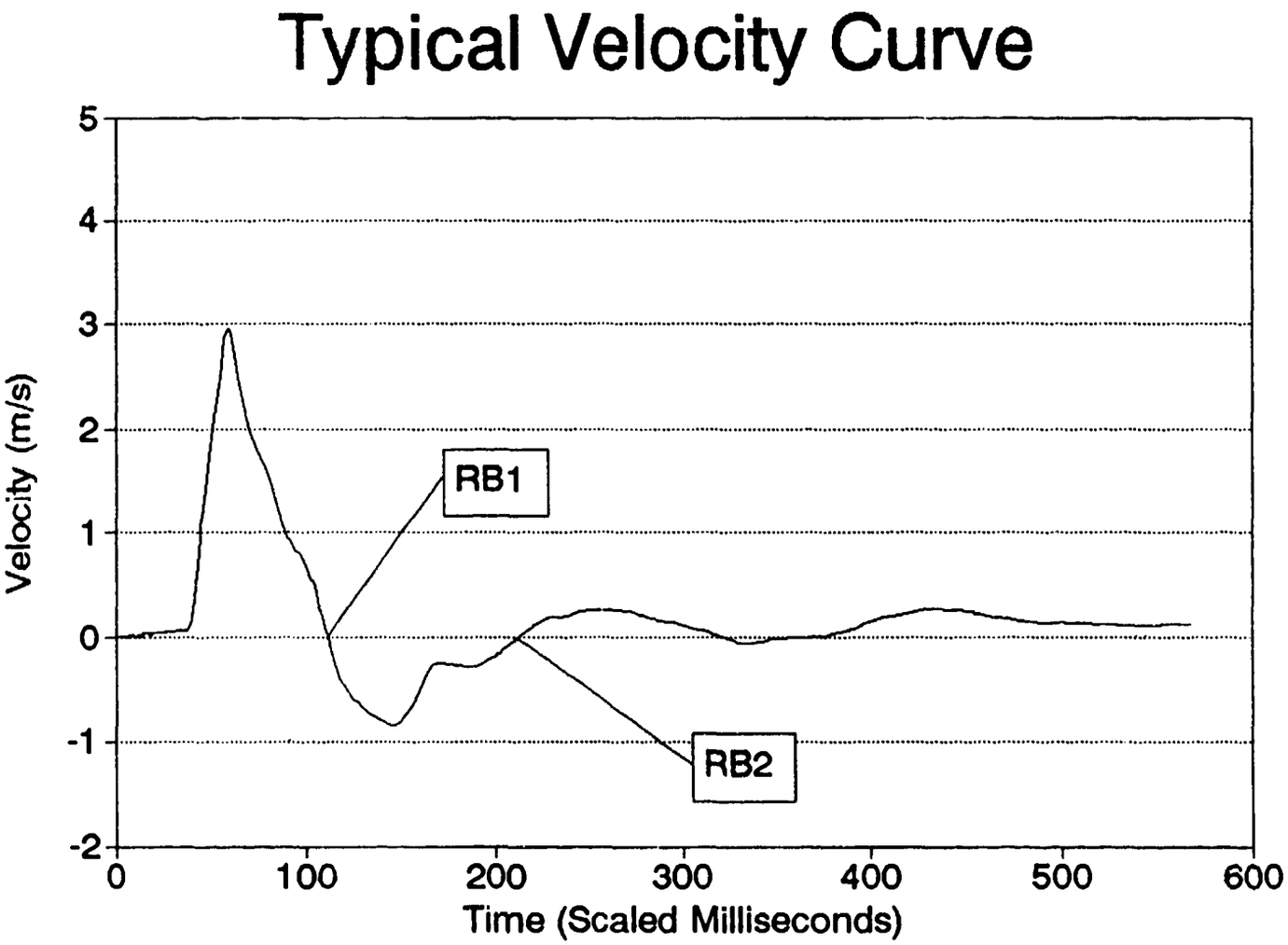
Typical Velocity Curve
Velocity (m/s)
5
4
3
2
1
0
-1
-2
0
100
200
300
400
500
600
Time (Scaled Milliseconds)
RB1
RB2

Figure 3.10

Rebound 1 Time Versus Range

Tunnel Tests

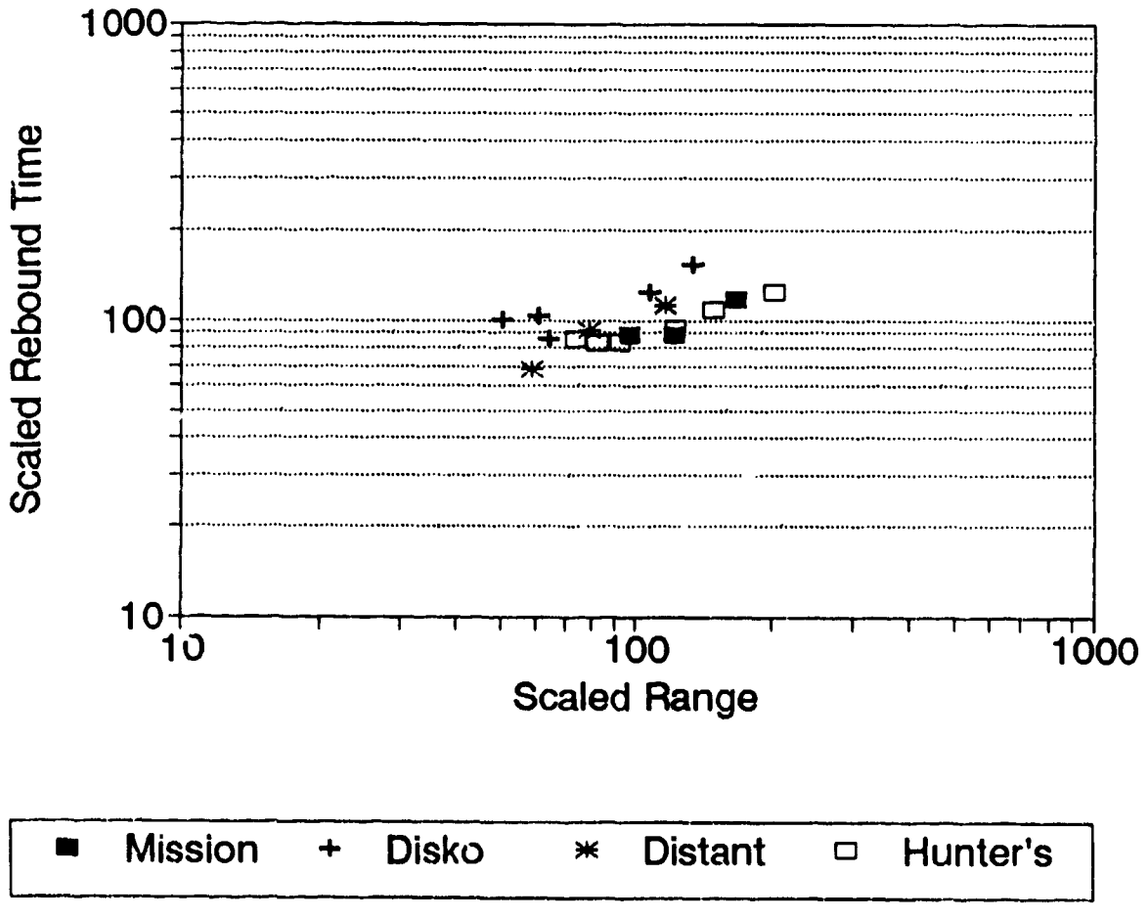

Figure 3.11a

Time Duration of Velocity Toward Source

Tunnel Tests

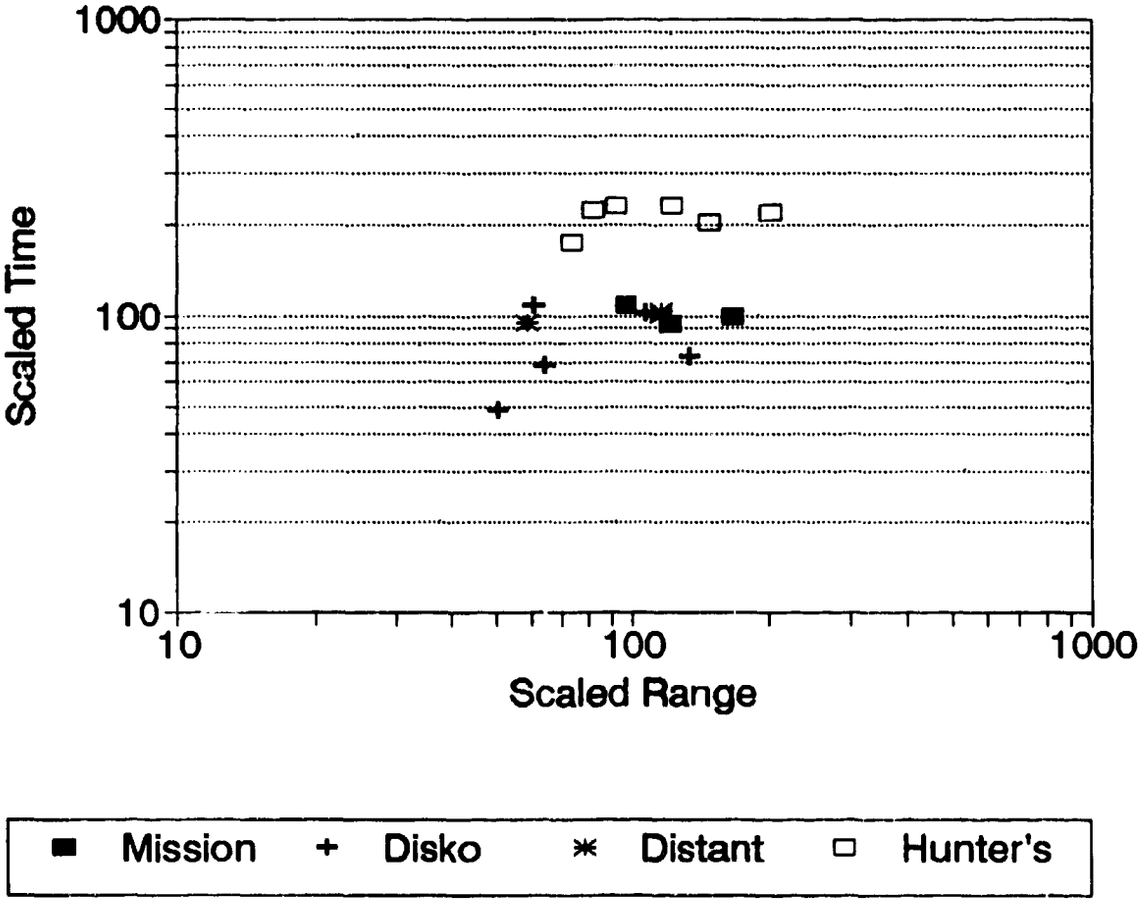

Figure 3.11b

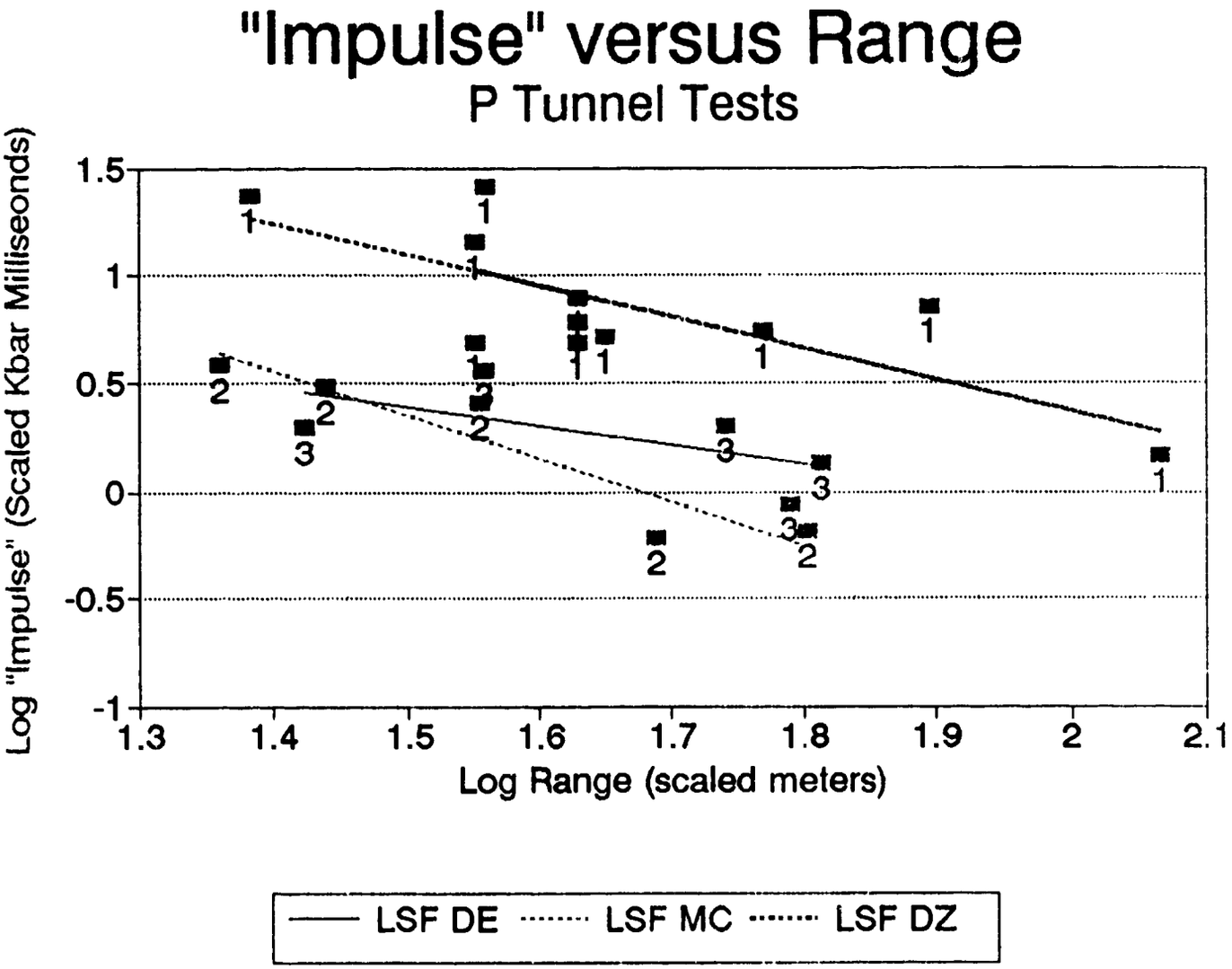
"Impulse" versus Range
P Tunnel Tests
Log "Impulse" (Scaled Kbar Milliseonds)
1.5
1
0.5
0
-0.5
-1
1.3
1.4
1.5
1.6
1.7
1.8
1.9
2
2.1
Log Range (scaled meters)
LSF DE
LSF MC
LSF DZ

Figure 3.12

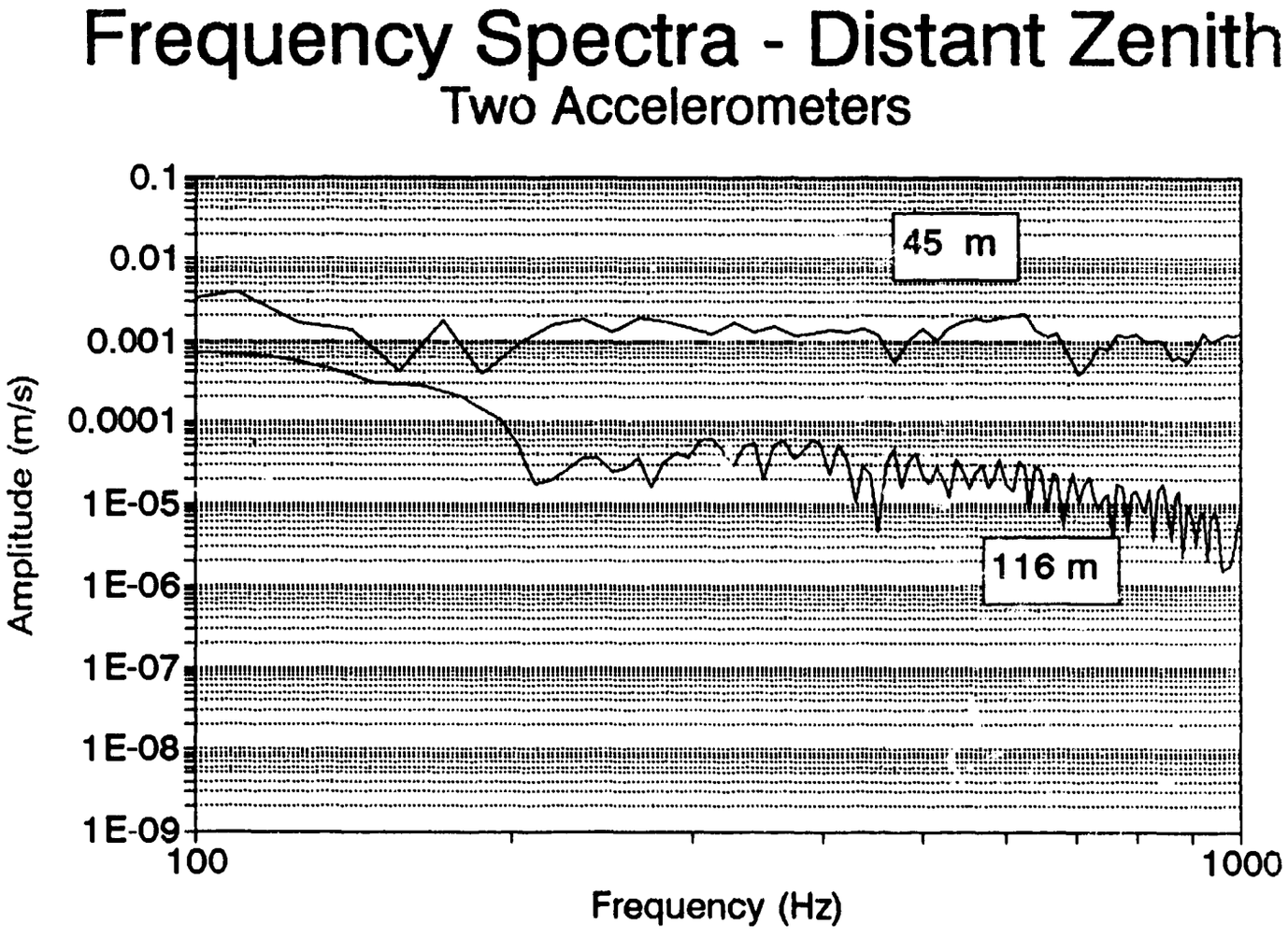
Frequency Spectra - Distant Zenith
Two Accelerometers
0.1
0.01
0.001
0.0001
1E-05
1E-06
1E-07
1E-08
1E-09
Amplitude (m/s)
45 m
116 m
100
1000
Frequency (Hz)

Figure 3.13

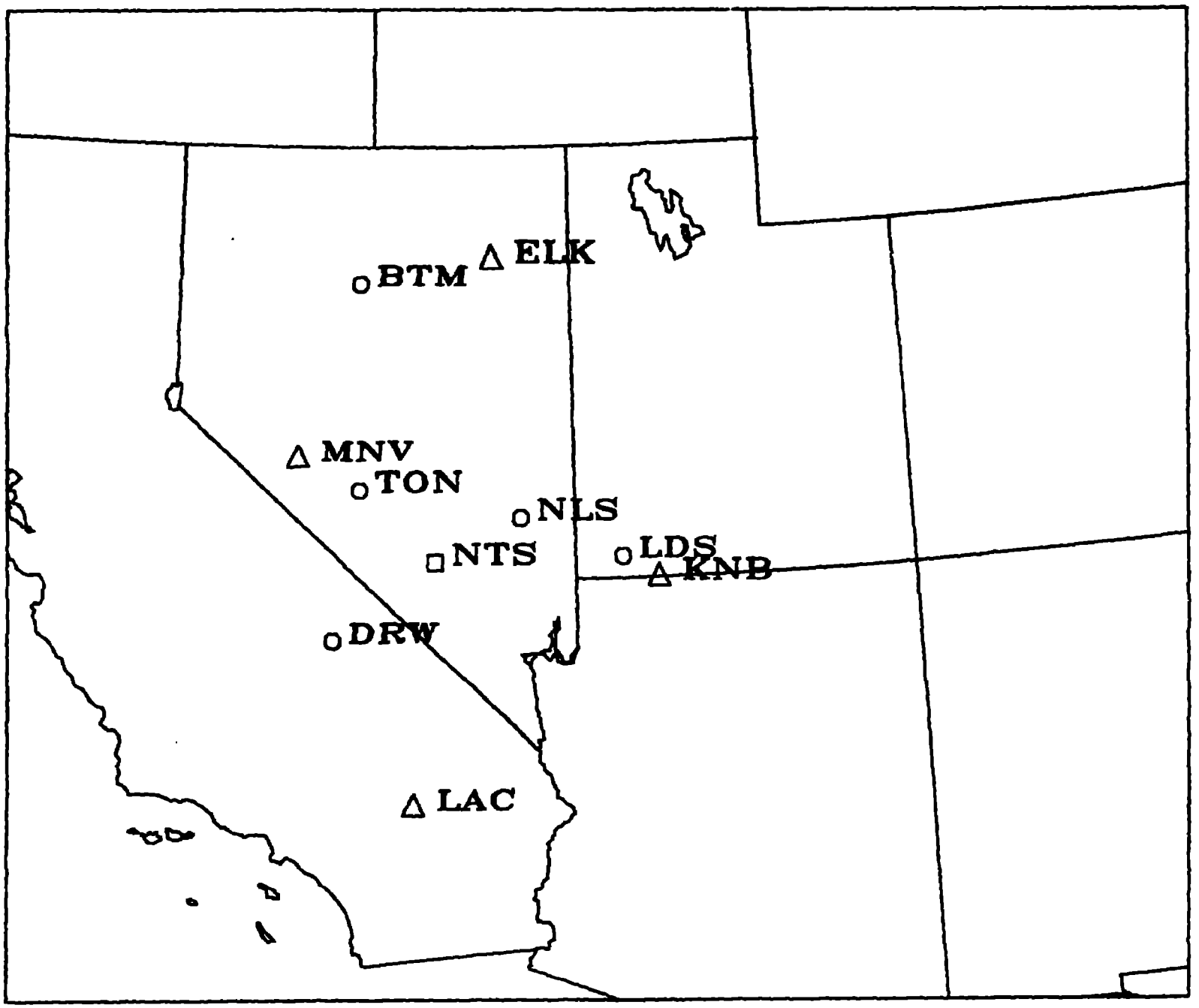

Figure 4.1